Short-range Forecasting Research

Short Range Forecasting Division
Scientific Paper No. 12

A NEW APPROACH TO SHALLOW FLOW OVER AN OBSTACLE

II Plane Flow over a Monotonic Mountain

by

A.S. Broad, D. Porter and M.J. Sewell

10 August 1992

Meteorological Office
London Road
Bracknell
Berkshire
RG12 2SZ
United Kingdom

ORGS UKMO S

National Meteorological Library
FitzRoy Road, Exeter, Devon. EX1 3PB

A NEW APPROACH TO SHALLOW FLOW OVER AN OBSTACLE

II Plane Flow over a Monotonic Mountain

by

A.S. Broad

Meteorological Office, Bracknell, RG12 2SZ

D. Porter and M.J. Sewell

Department of Mathematics, University of Reading,

Whiteknights, Reading RG6 2AX

10 August 1992

Abstract

The general results of Part I are applied to the problem of shallow flow over an obstacle in a single vertical plane, i.e. in which the conditions are independent of one horizontal coordinate. For a wide class of monotonic mountains, we obtain many new flows. These include steady continuous smoothly branched flows, in which the fluid speed and the free surface profile bifurcate smoothly at the apex of the mountain, unless the mountain is locally parabolic there. In the latter case the free surface bifurcation is known to be abrupt or sharp at the apex, but we show that this is the exception. We demonstrate that the fluid speed and free surface shape are sensitive to the mountain shape near the apex. Pseudo-steady flows, containing a bore travelling upstream from the obstacle, are exhibited. In some cases the bore serves to relieve what would otherwise be a blocked continuous flow. If the Froude number is not too large, the bore can lift the fluid so that it subsequently flows over the obstacle either freely or, if energy dissipation is minimized at the bore, with a bifurcation at the apex.

1. Introduction

In the first part of this work (Broad, Porter and Sewell (1991)), which will be referred to here as I, a new account is given of general local properties of shallow flows over an undulating, rigid bed. Constitutive surfaces are used to exhibit inherent relationships between physical variables, in advance of applying dynamical balance laws. The geometrical viewpoint implied by the constitutive surface approach allows the consequences of these laws to be clearly displayed, in the case of bores, for instance.

In this paper, the theory developed in I is illustrated by a straightforward direct application in which the shallow flow is one dimensional. That is, the flow is independent of one horizontal cartesian coordinate. We use terminology appropriate to the flow of air over mountains but our account applies equally to the flow of water above an uneven bed. One reason for our choice of emphasis is that the determination of atmospheric flow over a mountain, although a problem of long standing, is one which continues to attract attention.

The present contribution builds upon the geometrical structure which is given prominence in I. We do more than merely provide a fresh setting for the problem, however. We also give new results which substantially extend and amend previous work. This is true even though we use the simplest model of shallow flow, in which the fluid is assumed to have uniform density. More sophisticated models of atmospheric flows, in which the air has a given continuous or discrete stratification, have been considered and are described in some of the references given below. We restrict remarks on existing work to those aspects concerned with a single fluid of uniform density. It is worth noting, however, that in a two-layer fluid system in which the upper layer is infinite in extent, the lower layer behaves as a single fluid in a reduced gravity field.

The lower layer may also behave as a single fluid if the upper layer has finite depth and significantly less density; in this case the layers can be described as weakly coupled.

Long (1954) gave some discussion of what we would describe as the cross-section Q = constant of the surface in Q, h, d space depicted in Fig. 3 of I. In this influential paper, Long describes results of wave tank experiments simulating flow over an obstacle which is accelerated from rest up to a constant speed, in water initially at rest. He also provides a preliminary theoretical basis for the observed phenomena, using shallow water theory. Houghton and Kasahara (1968) extended Long's theoretical investigation by considering steady and pseudo-steady numerical solutions of the shallow flow equations. One of their key contributions is the construction of a flow classification diagram showing the type of solution which occurs when a given incoming flow encounters an obstacle of given maximum height. This diagram has subsequently been modified in content and interpretation by Long (1970), and by Baines and Davies (1980, pp. 238-239) who identified a phenomenon which they called hysteresis. This results from the existence of two possible solutions for the same assigned incoming flow and maximum obstacle height. Pratt (1983) describes a numerical experiment in which this "hysteresis" occurs and Baines (1984) identifies the analogous phenomenon in a physical experiment for a two layer model, with weak coupling in the sense described above.

Summaries of the early work in this area were given by Long (1972) and Huppert (1980), and the review article by Baines (1987) includes some later developments. Pratt (1984) gives the most explicit recognition that we have seen of the presence of an abrupt bifurcation of the free surface over a parabolic apex. Lawrence (1987) has described experiments involving steady flow over a fixed obstacle, with some analysis. He considers hydraulic jumps, but excludes bores.

In §2 we identify some cross sections of the constitutive surfaces which are appropriate for use in the study of one dimensional steady flows over an obstacle. We introduce a family of profiles representing various shapes of monotonic mountain with apex height a, in terms of which we define the notions of free flow, branched flow and blocked flow. This family of profiles is new in this context, and we exhibit steady continuous free flows over them. We also exhibit branched flows over them, and this is a possibility which the previous literature seems to have overlooked, except for the locally parabolic profile, which is evidently the only one to have been explicitly considered. In a steady branched flow, the free surface and speed, as continuous functions of horizontal distance, bifurcate at the apex. Moreover, the type of bifurcation is sensitive to the local obstacle profile shape. The bifurcation is abrupt in the parabolic case. For a flatter apex the bifurcation is smooth with a horizontal tangent, whereas for a sharper apex the bifurcation is smooth with a vertical tangent (subject to the limitations of shallow water theory, of course). This sensitivity is also new (see Figs. 3-9). The smooth bifurcations themselves have not been remarked upon before.

When a hypothesized incoming flow is blocked by the mountain, we give examples in §3 showing how this blocking can be relieved by a bore travelling upstream from the mountain. It is shown that the bore creates a flow over the apex which either branches there or, if more energy is dissipated at the bore, the outgoing flow passes freely over the apex without branching. New results are included here too. It is shown that there is a maximum supercritical Froude number above which blocked incoming flows can never be relieved by a bore in the way described.

Hydraulic jumps and bores can occur in a free or branched flow, just as an alternative, and we explore these in §§4 and 5. The examples

include a case in which two bifurcations at the apex are available to a supercritical incoming flow, one when it is branched without meeting a bore, and one after it meets a bore. A supercritical incoming flow can also be free or, after meeting a bore, branched at the apex. Such pairs of solutions extend the family of so-called "hysteresis" effects noted by the authors mentioned above.

In §6 we summarize our solutions, and give a classification diagram (Fig. 16) involving upstream bores which is much more comprehensive than any which is currently available. Particular downstream effects, such as lee jumps, can be analysed by the same methods. However, they require the specification of particular controls at a distance downstream, such as those different ones implied by the experiments of Long or Lawrence.

References back to equations, figures or sections in I will be indicated by a prefix, such as I(5) for equation (5) of I. The prefix will be omitted when referring to the present paper.

2. Steady Flow over a Monotonic Mountain

The properties deduced in I are completely general. That is, they apply to shallow flow over a continuous uneven bed of arbitrary shape extending in two horizontal dimensions; the flow may be steady or unsteady where it is continuous; and it may contain hydraulic jumps or bores which can be curved in plan view, and where energy is dissipated.

For the assumption of hydrostatic pressure to be appropriate we require that the characteristic horizontal length scale of the topography greatly exceeds its characteristic vertical length scale. We are therefore considering flows over obstacles which are long relative to the fluid depth and slowly-varying. In the illustrations we give, the horizontal and vertical length scales have been chosen in the interests

of clarity. Other scalings, conforming with the hydrostatic pressure assumption, are obviously possible. The semi-circular mountain, which is treated by some authors, has a fixed aspect ratio and so cannot be rescaled in such ways. It does not belong to the family (6) of profiles considered in this paper. In common with other authors, however, we assume that the earth's rotation is negligible and that the overall scale is consistent with this.

We now illustrate the general properties in I by a special case which has been studied before. We show in particular how the novel approach set out in §I3 brings new information and new viewpoints to that problem which augment the existing literature.

We consider flow with all properties independent of x_2, and write x in place of x_1 for simplicity. Then the given function $b(x)$ now specifies the bed profile $x_3 = b(x)$, and there is only one non-zero velocity component $u_1(x,t)$. With the foregoing assumptions, the whole of I still applies with fluid speed $u = |u_1|$ and $u_2 = 0$, so that $Q = |Q_1|$ and $Q_2 = 0$.

Wherever the flow is continuous I(30) and I(31) reduce to

$$\frac{\partial d}{\partial t} + \frac{\partial Q_1}{\partial x} = 0 , \qquad \frac{\partial u_1}{\partial t} + \frac{\partial e}{\partial x} = 0 . \tag{1}$$

Any regime of steady flow evidently possesses two integrals

$$Q = \text{constant} , \qquad e = \text{constant} \tag{2}$$

of (1) with respect to x. When the Q constant is nonzero we can choose $u = u_1 > 0$ without loss of generality, so that there is no stagnation point and the steady flow is in the direction of the positive x axis without reversal.

The viewpoint indicated after I(34) becomes especially appropriate in any such regime of steady continuous flow, because the values of Q

and e are now fixed by the dynamical equations, rather than merely by mathematical hypothesis. The value of $k = \frac{1}{g}\left(e - \frac{3}{2}(gQ)^{2/3}\right)$ in $I(33)_1$ is then also fixed.

The bed profile function $b(x)$ will contain its highest or apex value a (say) as a parameter, so that we can write it as $b(x,a)$. Then the constitutive relation I(35) becomes

$$b(x,a) = m(u) \qquad \text{where} \qquad m(u) = \frac{1}{g}\left(e - \frac{1}{2}u^2\right) - \frac{Q}{u} . \tag{3}$$

An example of this function $m(u)$ is shown in Fig. 1, for the particular parameter values $Q = 9$, $e = 7.5$, $g = 1$. This curve is a transcription of the cross section Q = constant of Fig. I2, using $h = e - gb$ from I(32) with e = constant to convert from the h,u plane.

Nondimensional alternative versions of $m(u)$ are

$$\frac{m\, e^{1/2}}{Q} = \frac{e^{3/2}}{gQ}\left[1 - \frac{1}{2}\left[\frac{u}{e^{1/2}}\right]^2\right] - \frac{e^{1/2}}{u} , \tag{4}$$

$$\frac{m\, g}{(gQ)^{2/3}} = \frac{e}{(gQ)^{2/3}} - \frac{1}{2}\left[\frac{u}{(gQ)^{1/3}}\right]^2 - \frac{(gQ)^{1/3}}{u} . \tag{5}$$

One could work with either of these functions of the differently non-dimensionalized speed variable $u/e^{1/2}$ or $u/(gQ)^{1/3}$, for any assigned value of the composite parameter $e/(gQ)^{2/3}$; and if the latter were 1.73 it would include more cases then our selected one of $Q = 9$, $e = 7.5$, $g = 1$. But an advantage of working with the dimensional function $m(u)$ of u itself is that this choice of variable need not be changed when we come to handle a bore, at which e and Q jump to new values.

Transcription of the cross-section Q = constant of Fig. I3, again

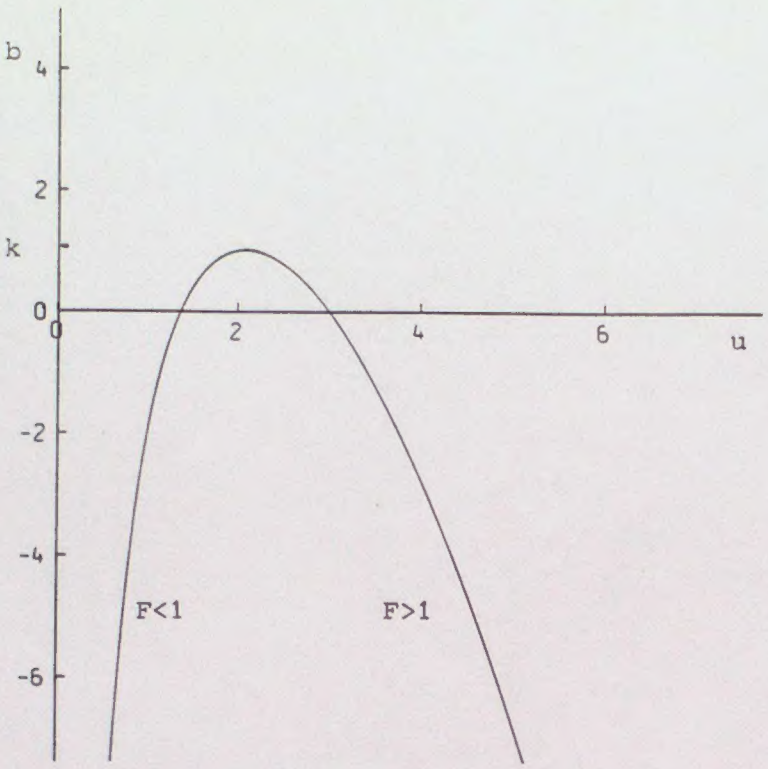

Fig. 1 b = m(u) for Q = 9, e = 7.5, g = 1.

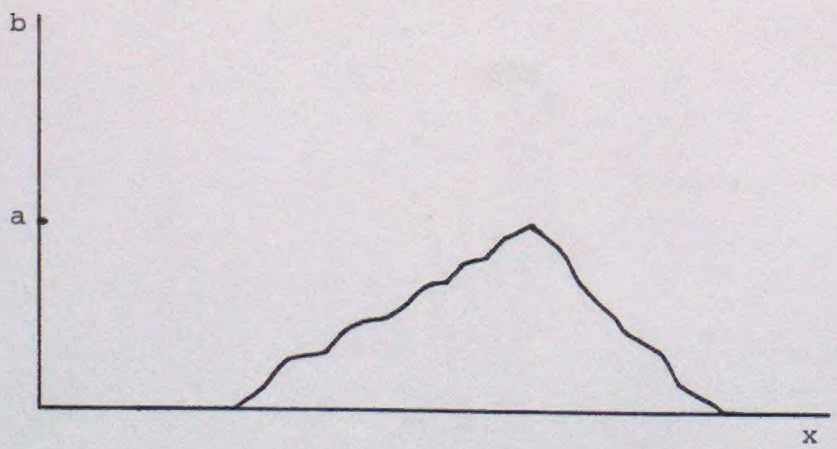

Fig. 2 Monotonic mountain $x_3 = b(x)$.

using $h = e - gb$ with e = constant, will give a dependence of b upon d which is similar to Fig. 1, having the same maximum value k, but with the subcritical and supercritical parts interchanged. Similar transcription of the cross section Q = constant of Fig. I4 will give a cusped dependence of b upon P, also having the maximum value k.

Thus far the bed function might have several different local maxima. The principles of our analysis will be sufficiently well illustrated by considering an obstacle with a single local apex or top at $x = a$. Thus we assume that the bed function $b(x)$ is a continuous function which rises monotonically from zero to a single top and then falls monotonically to zero again. Fig. 2 illustrates such a function, which we can call a monotonic mountain. The mountain need not be convex or smooth or symmetric about its apex, as it is often portrayed in the literature. A simple model of a monotonic mountain is

$$b(x) = \begin{cases} a\left[1 - \left[\frac{v-x}{v+\ell}\right]^{\sigma}\right] & -\ell \le x \le v \\ a\left[1 - \left[\frac{x-v}{\ell-v}\right]^{\sigma}\right] & v \le x \le \ell \end{cases} \qquad (6)$$

with $b(x) = 0$ where $|x| \ge \ell$. Here a, ℓ, v and σ are assignable parameters. We assume $\ell > |v|$ and $\sigma > 0$. When $a \ge 0$ we can interpret a as the height of the top of the mountain, but we can also allow $a < 0$ incidentally, in which case (6) models a depression in an otherwise flat bed. The length of the mountain or depression is 2ℓ, and the value of v/ℓ indicates its asymmetry. The value of $1/\sigma$ is a measure of the sharpness of the top. The slope of (6) at $x = \mp \ell$ is

$a\sigma/(\upsilon \pm \ell)$, so that there is a slope discontinuity at the roots of the obstacle, where it joins the flat bed. One could smooth out these latter discontinuities, of course, but we shall not do that, because we are more concerned to examine the effect of different top shapes. Over all x our function $b(x)$ is therefore piecewise C^1, except that it has a spiked top (infinite slope) if $\sigma < 1$. The bilinear mountain $\sigma = 1$ has a finite slope discontinuity at the top. Unsymmetric examples of (6) with $\upsilon = 0.5\ell$ are displayed at the bottom of Figs. 3-8 for $\sigma = 0.5,\ 1,\ 1.5,\ 2,\ 3,\ 10$ and for the particular value k of a. Other choices of a would merely change the height of the obstacle without altering its asymmetry or sharpness.

The constitutive relation $(3)_1$ shows how fluid speed u must vary with spatial location x for each a. The form of this relation will depend crucially on whether the maximum value k of $m(u)$ in Fig. 1 is greater or less than the obstacle apex height a. The relation $(3)_1$ could be rewritten to express a as a function $a(x,u)$, each of whose contours $a(x,u) = \text{constant}$ represents the relation between u and x for the chosen value of a. Three cases present themselves for any obstacle shape (not only (6)) having apex height a, which we call

$$(\alpha)\quad \underline{\text{free flow}} \qquad a < k\ , \tag{7}$$

$$(\beta)\quad \underline{\text{branched flow}} \qquad a = k\ , \tag{8}$$

$$(\gamma)\quad \underline{\text{blocked flow}} \qquad a > k\ , \tag{9}$$

for the given values of Q and e characterizing the steady flow.

Similar manipulations can be carried out to obtain relations between P and x, between d and x, and hence between s and x from $s = d+b$.

We choose the values $Q = 9$ and $e = 7.5$ in (2) as being adequately representative. From Fig. I(6) with $g = 1$ they imply two flows over the flat part of the bed with Froude numbers $F = 0.54$ and 1.73, the latter having $u = 3$ and $d = 3$.

For each of the examples of (6) with $\nu = 0.5\ell$ and $\sigma = 0.5,\ 1,\ 1.5,\ 2,\ 3,\ 10$ eleven pairs of calculated contours $a(x,u) = \text{constant}$ are displayed at the top of Figs. 3-8 respectively. The contour key in Table 1 lists their a values in the range $-0.8 \leq a \leq 2.8$. The corresponding free surface profiles $x_3 = s(x)$ are displayed in the centre of Figs. 3-9.

contour label	1	2	3	4	5	6	7	8	9	10	11
a value	-0.8	-0.4	0	0.4	0.8	1.01	1.2	1.6	2.0	2.4	2.8
type	α	α	α	α	α	β	γ	γ	γ	γ	γ

Table 1 Contour key for Figs. 3-9.

For each value of $a < k$ there is a pair of α contours, one with $F < 1$ and one with $F > 1$, in every diagram. Each such $u(x)$ and $s(x)$ is a single valued function of x which is defined for all x, so that the flow is <u>free</u> in the sense of not being blocked. We display five pairs of α contours, for $-0.8 \leq a \leq 0.8$; two pairs model flow over a depression, one over a completely flat bed, and two pairs model

free flow over an obstacle. The properties shown graphically can be readily confirmed and supplemented analytically. For example, slope discontinuities of $u(x)$ and $s(x)$ coincide with those of $b(x)$ at $x = \pm \ell$ for all σ, and at the top $x = v$ for $\sigma = 1$. Also at the top, $du/dx = 0$ if $\sigma > 1$; but if $\sigma < 1$ there is a cusp with $dx/du = 0$, and $d^2x/du^2 = 0$, finite, ∞ if $\sigma <$, $=$, > 0.5 respectively.

For the value $a = k$, in every diagram there is one pair of β contours, which meet at the top where $F = 1$, and the slopes of $u(x)$ and $s(x)$ there also depend significantly on the value of σ. We give some analytical discussion below. For example, this slope is infinite for a bilinear or spiked mountain ($\sigma \leq 1$), finite and non-zero for a parabolic mountain ($\sigma = 2$) and discontinuous in the unsymmetric case $v \neq 0$, and zero if $\sigma > 2$, as for a cubic mountain ($\sigma = 3$). As x passes through the top, both the subcritical and supercritical β contour on the left can branch to follow either the subcritical or the supercritical β contour on the right. The branching is smooth for all σ except $\sigma = 2$. This bifurcation is the reason for our name <u>branched</u> flow, and we have not seen the smooth bifurcations exhibited elsewhere. The β contours have $a = 1.01$ as Table 1 indicates. We have chosen the sample mountain displayed in the Figures to have this apex height. This means that in Figs. 3-9 the distance between the free surface β contours and the mountain profile is the actual depth in that case.

For each $a > k$ there is a pair of γ contours in every diagram having turning points at $F = 1$, which cannot meet at the top, and we display five such pairs for $1.2 \leq a \leq 2.8$. Therefore, in a finite x neighbourhood of the top there are no u or s values. This is the well recognised <u>blocked</u> flow. The putative steady flow $u(x)$ on the

left cannot exist alone, because it is not defined for all x; and nor could the corresponding one on the right if the flow came from there, or if the unsymmetric mountain were turned round. The putative flow is blocked by the obstacle at a location represented by the turning point of each τ contour, and if it exists at all, that could only be in association with other flows which we have not yet examined. The top is high enough to block the steady flow under consideration, at a determinable location where $F = 1$ part way up the mountain side.

The nature of the bifurcation of the β contours can be explored along the following lines. Suppose that the β contour in the neighbourhood of the top can be equivalently written

$$b(x) = m(u) \qquad \text{or} \qquad u = u(\epsilon) \ , \quad x = x(\epsilon) \tag{10}$$

in terms of a path parameter ϵ, for (6) or any other obstacle profile. Let a prime denote ϵ differentiation. Two differentiations along the β contour gives

$$\frac{db}{dx} x' = \frac{dm}{du} u' \ , \tag{11}$$

$$\frac{d^2b}{dx^2} x'^2 + \frac{db}{dx} x'' = \frac{d^2m}{du^2} u'^2 + \frac{dm}{du} u'' \ . \tag{12}$$

From $(3)_2$ we find

$$\frac{dm}{du} = -\frac{u}{g}\left[1 - \frac{1}{F^2}\right] , \quad \frac{d^2m}{du^2} = -\frac{1}{g}\left[1 + \frac{2}{F^2}\right] \tag{13}$$

Therefore, derivatives at the top, where $F = 1$, from either side, satisfy

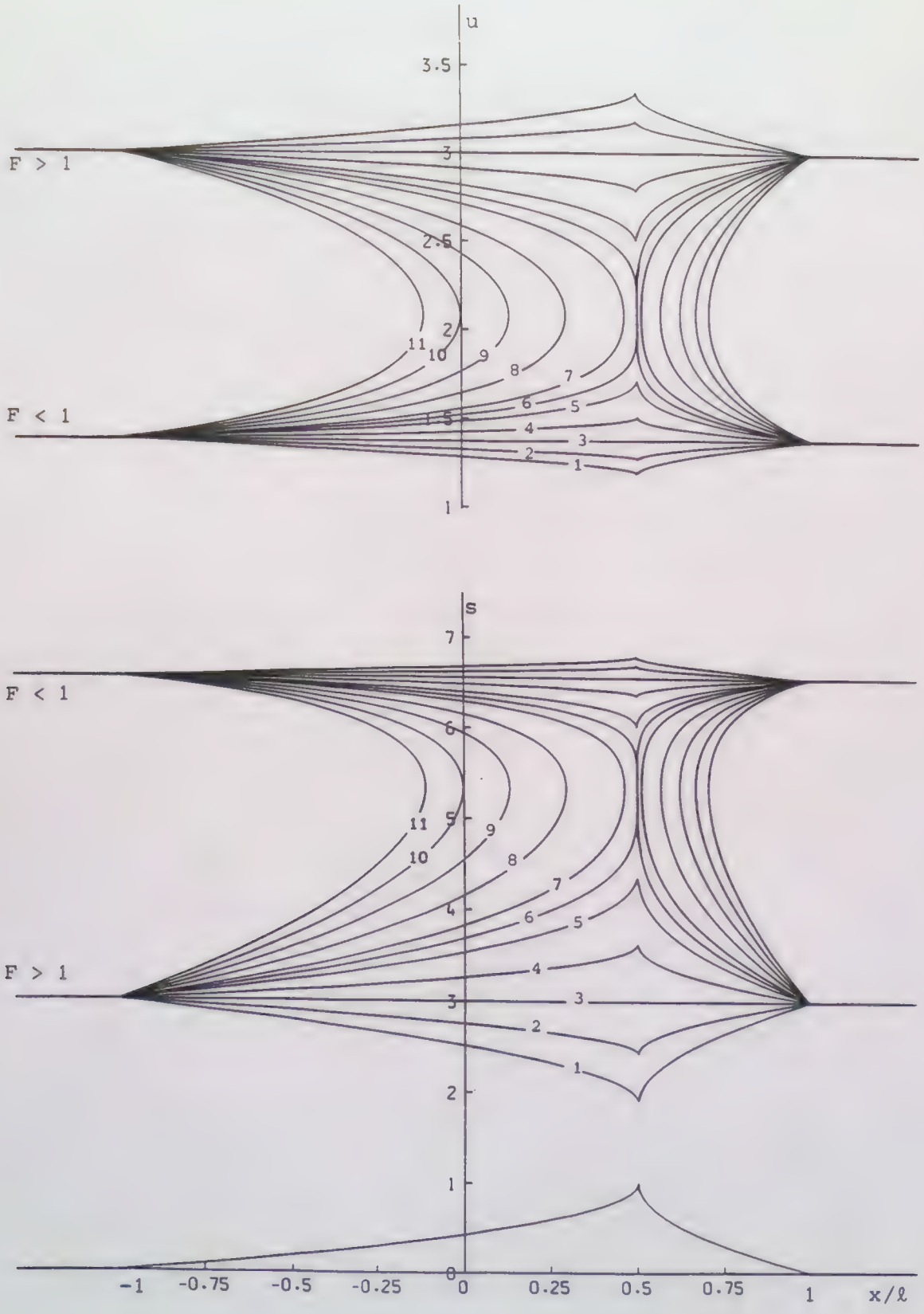

Fig. 3 Contours of speed a(x,u) = constant and profiles of free surface a(x,s) = constant and mountain shape (6) for $\sigma = 0.5$, $\nu/\ell = 0.5$, $Q = 9$, $e = 7.5$, $g = 1$.

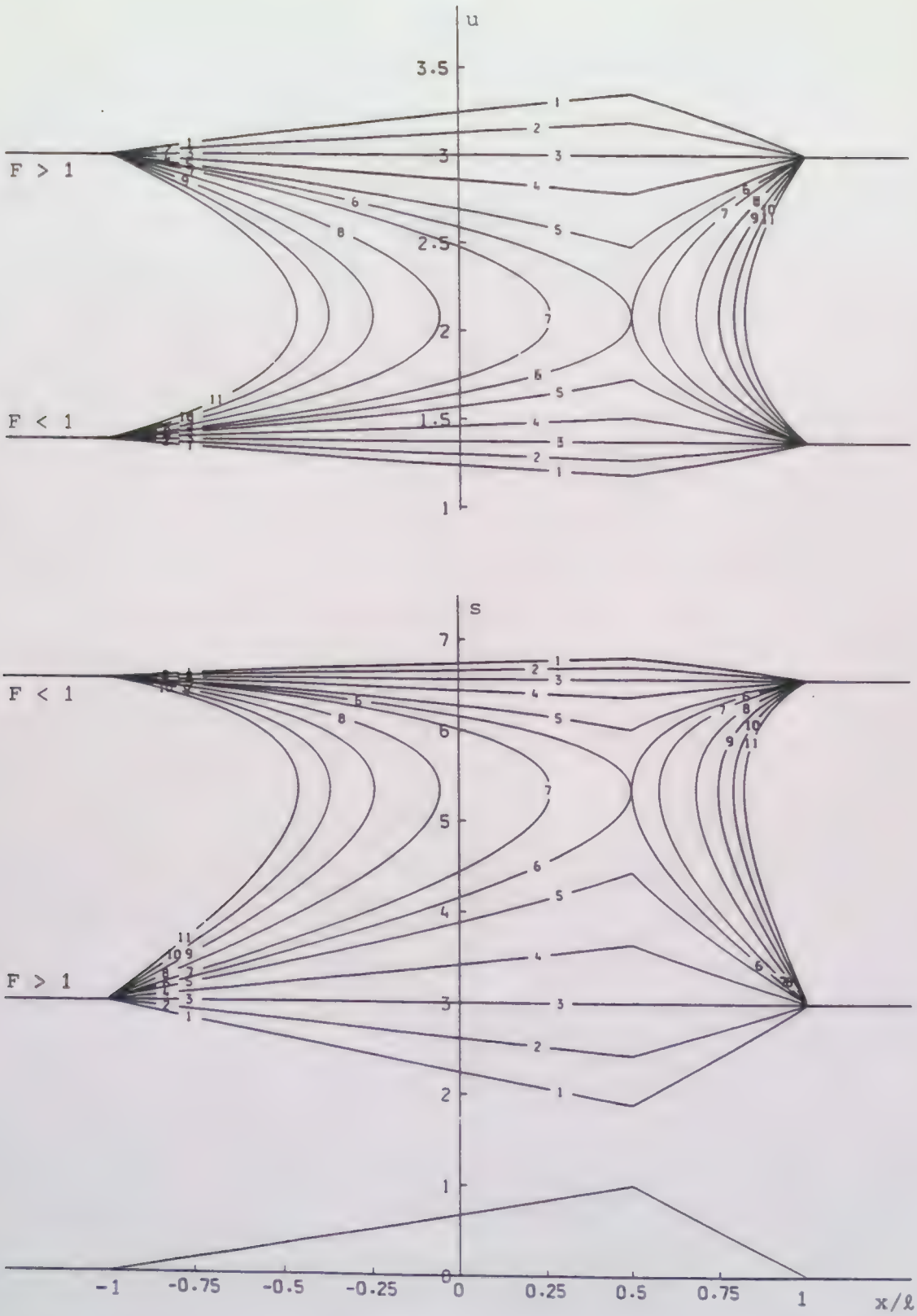

Fig. 4 Contours of speed a(x,u) = constant and profiles of free surface a(x,s) = constant and mountain shape (6) for $\sigma = 1$, $\nu/\ell = 0.5$, Q = 9, e = 7.5, g = 1.

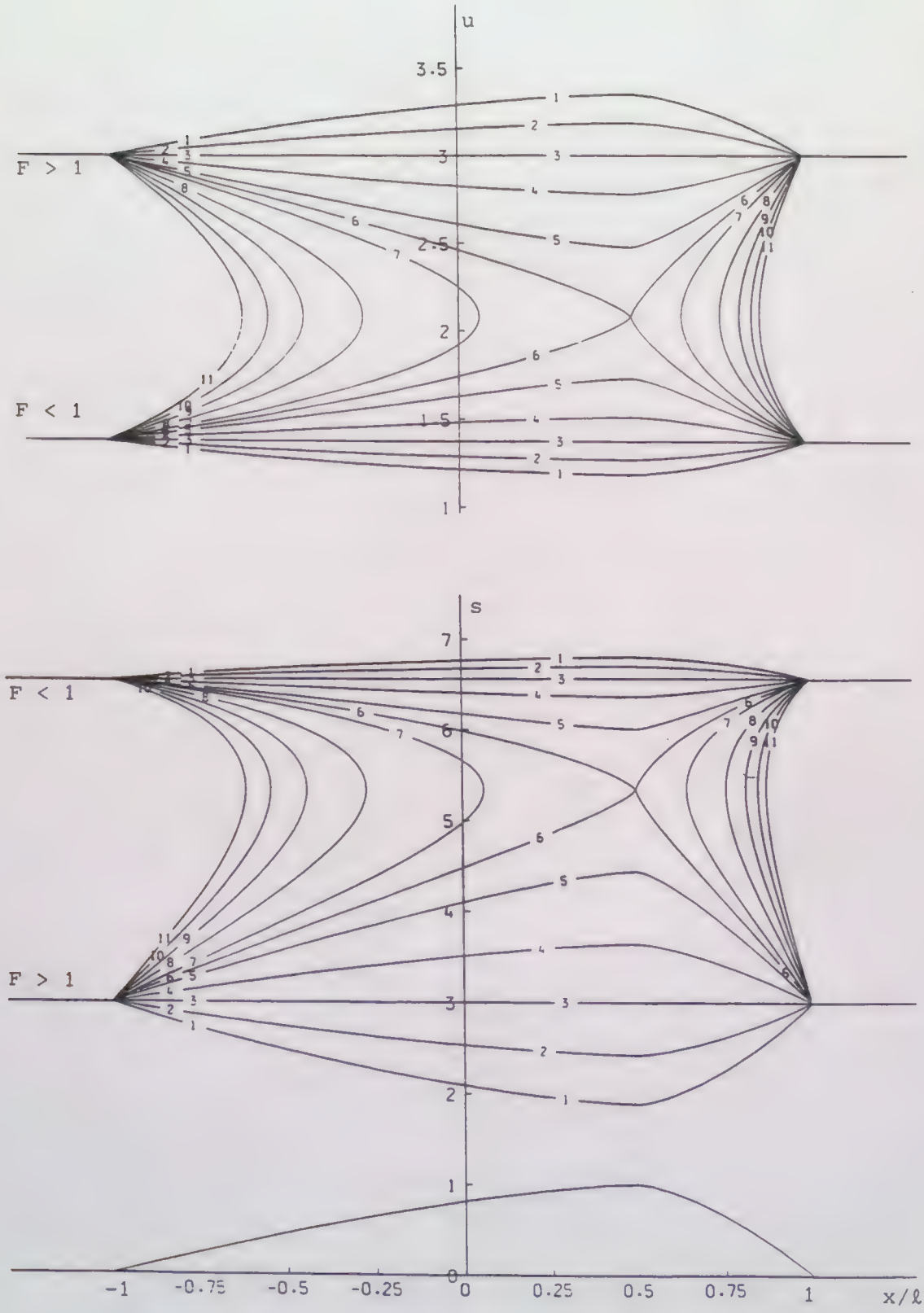

Fig. 5 Contours of speed a(x,u) = constant and profiles of free surface a(x,s) = constant and mountain shape (6) for $\sigma = 1.5$, $v/\ell = 0.5$, $Q = 9$, $e = 7.5$, $g = 1$.

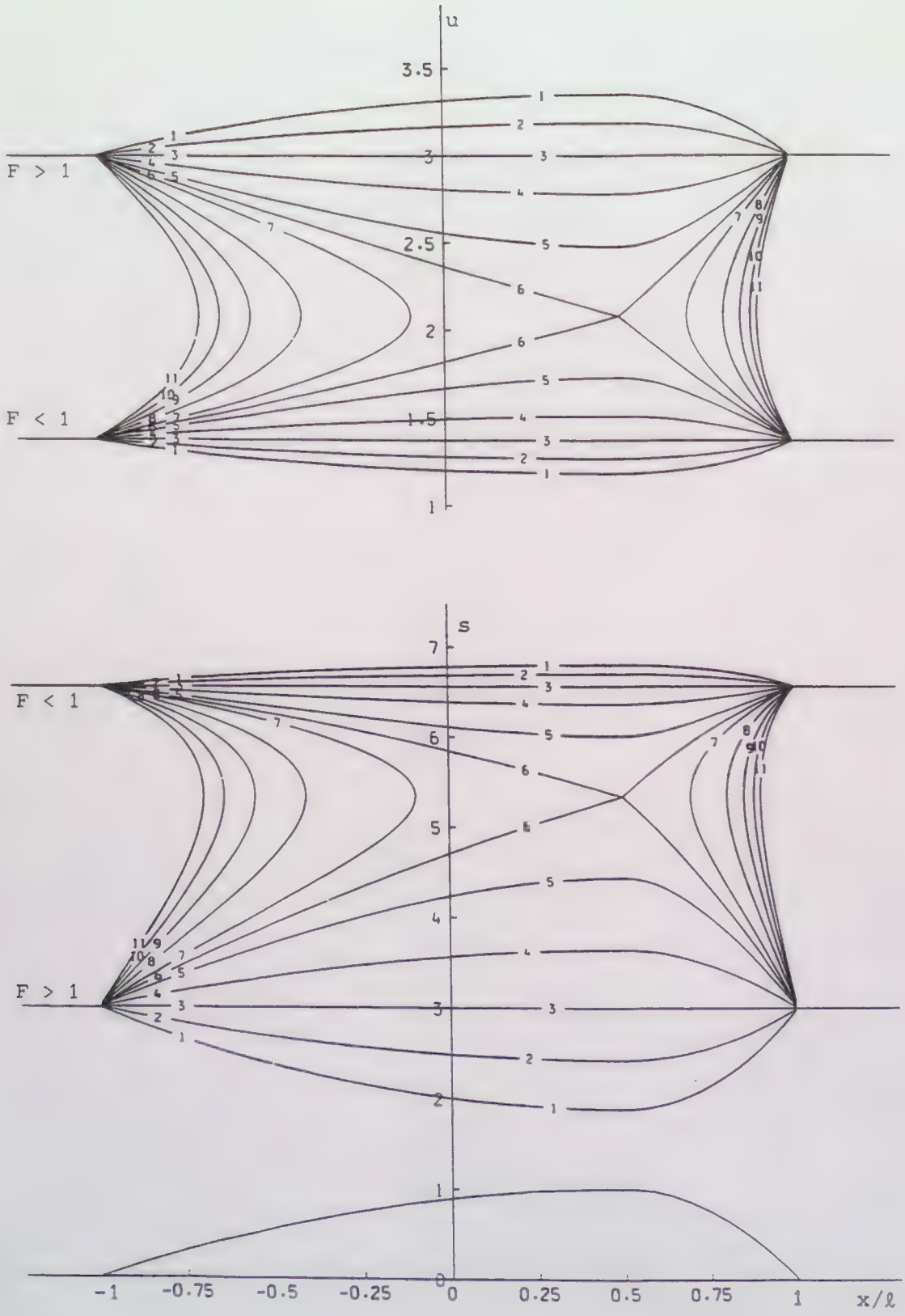

Fig. 6 Contours of speed $a(x,u)$ = constant and profiles of free surface $a(x,s)$ = constant and mountain shape (6) for $\sigma = 2$, $\nu/\ell = 0.5$, $Q = 9$, $e = 7.5$, $g = 1$.

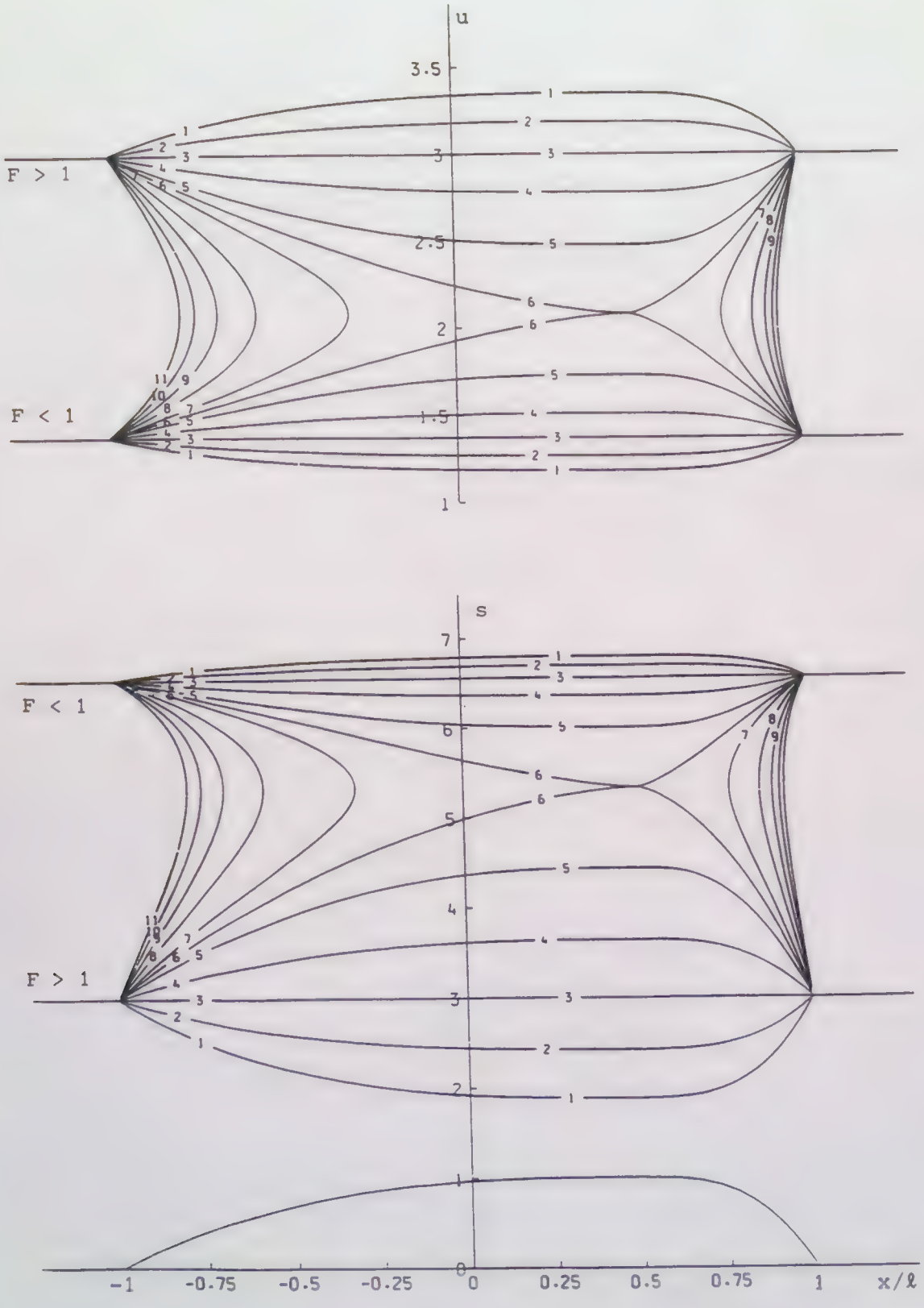

Fig. 7 Contours of speed $a(x,u)$ = constant and profiles of free surface $a(x,s)$ = constant and mountain shape (6) for $\sigma = 3$, $\upsilon/\ell = 0.5$, $Q = 9$, $e = 7.5$, $g = 1$.

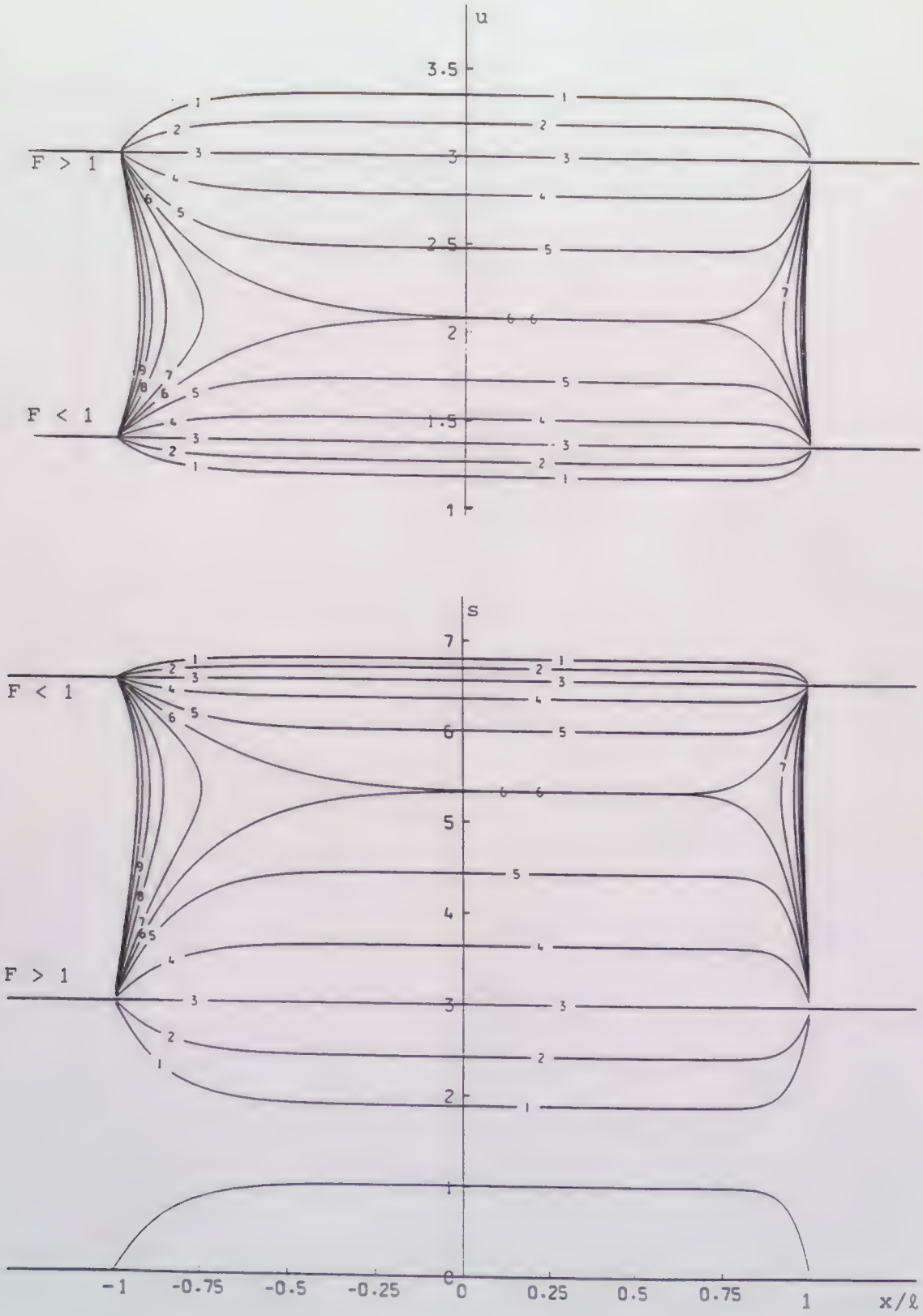

Fig. 8 Contours of speed a(x,u) = constant and profiles of free surface a(x,s) = constant and mountain shape (6) for $\sigma = 10$, $\nu/\ell = 0.5$, Q = 9, e = 7.5, g = 1.

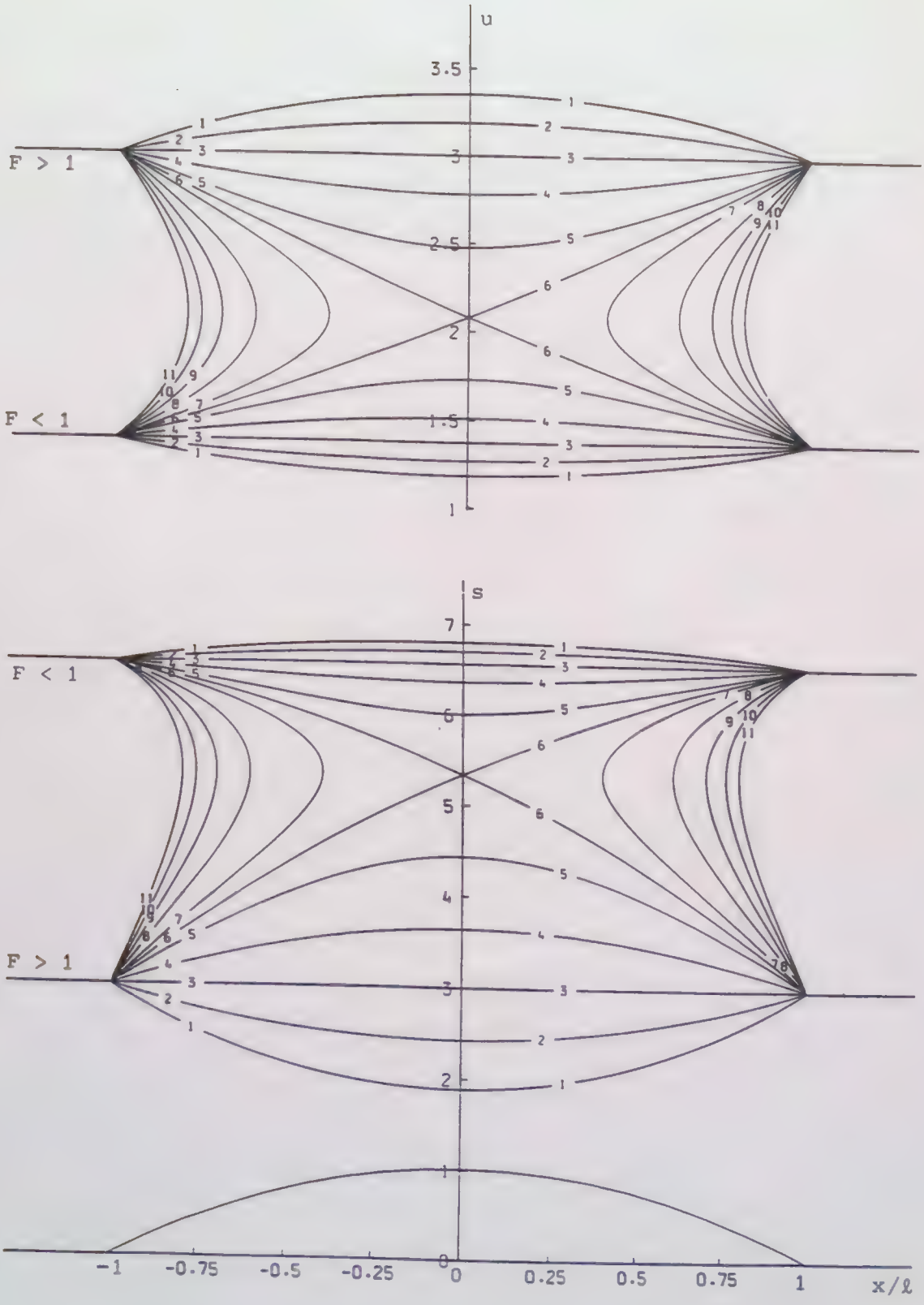

Fig. 9 Contours of speed a(x,u) = constant and profiles of free surface a(x,s) = constant and mountain shape (6) for $\sigma = 2$, $\nu = 0$, $Q = 9$, $e = 7.5$, $g = 1$.

$$\frac{db}{dx}\,x' = 0\,, \qquad \frac{d^2b}{dx^2}\,x'^2 + \frac{db}{dx}\,x'' = -\frac{3}{g}\,u'^2\,, \tag{14}$$

assuming u' and u'' are finite. It is important to recognise that these formulae apply not only to two-sided derivatives, but also to one-sided derivatives.

For a sharp top where $db/dx \neq 0$ and is finite from either side, if d^2b/dx^2 is finite (14) implies $x' = 0$ and

$$\frac{db}{dx}\,x'' = -\frac{3}{g}\,u'^2\,. \tag{15}$$

The right side is negative if $u' \neq 0$, which would be the case for a parametrization which is regular in the sense that $x'^2 + u'^2 = 1$. Then we can choose $\epsilon = u$, whence (15) shows that d^2x/du^2 has the opposite sign to that of db/dx, as Fig. 4 illustrates.

For a smooth top $db/dx = 0$, so that $(14)_1$ permits $x' \neq 0$. When x'' is finite $(14)_2$ then implies

$$\frac{d^2b}{dx^2}\,x'^2 = -\frac{3}{g}\,u'^2\,. \tag{16}$$

If d^2b/dx^2 is infinite at the top (as it is for (6) when $1 < \sigma < 2$), then (16) implies $x' = 0$ and we can choose $\epsilon = u$ for a regular parametrization, so that $dx/du = 0$ (as Fig. 5 illustrates with $\sigma = 1.5$ in (6)).

If d^2b/dx^2 is finite at a smooth top (in (6) for $\sigma > 2$ it is zero, and for $\sigma = 2$ it is finite, non-zero and (if $v \neq 0$)

discontinuous), we can choose $\epsilon = x$ for a regular parametrization, so that

$$\frac{du}{dx} = \pm \left[-\frac{g}{3} \frac{d^2b}{dx^2} \right]^{1/2} . \qquad (17)$$

Hence for $\sigma > 2$, such as the cubic mountain $\sigma = 3$ in Fig. 7, the β contours have a common horizontal tangent at the top. For a parabolic mountain $\sigma = 2$, however, the β contours reach the top at a finite non-zero angle from either side, as Fig. 6 shows. In the symmetric ($v = 0$) parabolic case the β contours cross at the top at a finite angle as shown in Fig. 9.

Evidently, when we think of a as a varying parameter, the surfaces $a = a(x,u)$ and $a = a(x,s)$ in Figs. 3-9 all have a ridge-line or fold where $F = 1$, and the α contours $a = \text{constant}$ along their flanks represent the two free flows, one subcritical and one supercritical, which are possible for the given Q and e. The saddle point of each surface is the bifurcation point of the branched flows possible when $a = k$.

The repetition of certain errors which can be found in the previous literature on steady continuous flows indicates that a proper understanding of even that relatively simple case has not yet been reached. Free surface profiles are commonly drawn as smooth curves, even at points above the non-smooth join of a convex obstacle to a flat bed, such as the roots of a parabolic obstacle. Fig. 9 gives the correct picture in that case, as does Fig. 1 of Pratt (1984) which is exceptional in being free from the stated errors. Shallow water theory predicts, as our analysis shows, that there must be a jump in the slope of the free surface wherever there is a jump in the slope of the obstacle profile,

and also (for the β contour) where there is a jump in top curvature of the smooth parabolic obstacle. Physical intuition tells us, of course, that a real free surface cannot have a slope discontinuity, but the explanation of that must lie outside shallow water theory per se. A more serious and mathematical error is found in the discussion of what we have called β contours over the top of a symmetric parabolic obstacle. One of the sign options in (17) is omitted, associated with a lack of appreciation that one-sided derivatives apply, and the conclusion is drawn that the β contour is smooth at the top, and therefore that the flow must pass either from subcritical to supercritical, or from supercritical to subcritical. This is not a valid conclusion from a purely local analysis. The possibility of bifurcation is thereby suppressed, again perhaps on the purely intuitive grounds that the β contours of free surface, speed and depth cannot have slope discontinuities. Again, however, there is nothing in the shallow water theory itself which justifies this suppression, as the left-right symmetry of the contour diagrams for $v = 0$ also suggests. They give a flow pattern which would not be altered if the flow were reversed, i.e. if we had chosen $u = - u_1 > 0$ after (2). Flow following a β contour may therefore also go from subcritical to subcritical as the top is passed, or from supercritical to supercritical, as far as these local considerations alone can discern. Gill (1977) considers a lee hydraulic jump associated with such a contour, for a symmetric parabolic obstacle only.

In the case of an asymmetric parabolic obstacle the β contour necessarily has a slope discontinuity at the top, as Fig. 6 shows, even when the transition is from subcritical to supercritical, or the reverse.

Also, at tops which are smoother than parabolic in the sense of $\sigma > 2$, the β contours have a common horizontal tangent at the top. In that case no transition between them is abrupt, so even the intuitive argument that a slope discontinuity is to be avoided where possible is not available for $\sigma > 2$, as Figs. 7 and 8 show. This emphasizes that other reasons must be sought to discriminate between the bifurcation possibilities at the top, such as a stability analysis (cf. Pratt, 1984).

We are not aware that the differences in flow patterns and bifurcation diagrams exhibited here for sharp and the various smooth obstacles have ever been demonstrated.

Incoming steady flow with constants Q and e can only follow a β contour in the exceptional circumstance when it encounters an obstacle whose top height is given exactly by $a = k$. There is then certainly the possibility that subcritical incoming flow can become supercritical outgoing flow. This is a possible model, among others, for the phenomenon of severe lee-slope windstorms, and a comparative study of the literature on these has been made by Durran and Klemp (1987). Our analysis shows that, for this model, the rise in velocity at the top would be much greater for a sharp top than for a smooth one, because of the vertical tangent to the β contours in Fig. 4, say. Smooth tops have $u(x)$ β-tangents with finite or zero slope, just as in Figs. 6 and 7 for parabolic and cubic obstacles. It would be interesting to know whether observational data offers any correlation between the strength of lee-slope winds near the top and the sharpness or smoothness there.

3. Relief of Blocking: Pseudo-steady Flow with a Bore

Turning now to blocked flows, the question arises whether a steady blocked flow on one side of an obstacle can coexist with another steady free flow passing over the obstacle, with a transition between two such continuous flows occurring at a bore or hydraulic jump.

Theorem 1

Blocking cannot be relieved purely by a hydraulic jump.

Proof

A hydraulic jump requires continuous Q, by I(40). Consider a steady flow coming in from the left with constants $Q > 0$ and e_-, passing through a hydraulic jump, and going out to the right with constants Q and e_+. From I(61) we should have $e_+ < e_-$. But if the incoming flow is blocked and the outgoing flow is free or branched, (7)-(9) give

$$e_+ \geq ga + \frac{3}{2}(Qg)^{\frac{2}{3}} > e_- \ . \tag{18}$$

The contradiction establishes the result. □

We now consider a steady continuous flow approaching the monotonic mountain from the left with constants $Q_- > 0$ and e_-, and either subcritical or supercritical, but blocked. The maximum height which the flow could reach up the mountain is therefore

$$k_- < a \ , \qquad \text{where} \quad k_- = \frac{1}{g}\left[e_- - \frac{3}{2}(gQ_-)^{\frac{2}{3}}\right] \ , \tag{19}$$

from (9). The flow could never proceed beyond the location defined by the turning point of the γ contour on the left of the crest associated with that value of k_- in Fig. 1, as illustrated for various obstacle shapes in Figs. 3-9.

In view of Theorem 1, we next enquire whether a bore can be the transition between the stated flow on the left, and another steady continuous flow on the right having constants $Q_+ > 0$ and e_+ satisfying

$$k_+ \geq a \ , \qquad \text{where} \quad k_+ = \frac{1}{g}\left[e_+ - \frac{3}{2}(gQ_+)^{2/3}\right] \ , \tag{20}$$

so that by (7) or (8) this second flow passes over the obstacle either freely or with a bifurcation at the top.

Thus we seek a solution in which the particle motion is to the right on <u>both</u> sides of the bore. If the bore were to reverse the direction of motion of the particle, or stop it, this would sustain the blocking in the sense that the particle would not move nearer the mountain. We choose the normal unit vector $\underline{m}$ to the bore in the positive x direction, so that from I(72) $\hat{F} = F > 0$ on both sides of the bore.

We also seek a bore travelling to the left $(C < 0)$, because if $C > 0$ the bore would run up against the mountain, and such a solution could not be convincingly described as a relief of blocking.

Then referring to the central part of Figs. I8 and I9 and Theorem I12(ii), we are seeking the type of bore which meets the particles such that

$$u_- > u_+ > 0 > C \tag{21}$$

with $d_- < d_+$. The jump conditions I(40) and I(42) become

$$\frac{Q_+ - Q_-}{d_+ - d_-} = \frac{P_+ - P_-}{Q_+ - Q_-} = C \tag{22}$$

for normal transit of this type, since $\underline{m}.\underline{Q} = Q$ on both sides of the bore. It follows that

$$Q_+ < Q_- \quad \text{and} \quad P_+ > P_- \ . \tag{23}$$

The contradiction which proves Theorem 1 is avoided when $C < 0$ because I(61), (19), (20) and (21) imply

$$\frac{3}{2}\left[(gQ_+)^{2/3} - (gQ_-)^{2/3}\right] < e_+ - e_- < C(u_+ - u_-) \ . \tag{24}$$

The left side is negative by $(23)_1$, and the right side is positive by (21), instead of both being zero as they are when $C = 0$.

The next Theorem describes bores which can effect the transition, at any location over the flat plain to the left of the mountain, between the hypothesized steady flows. Because $b = 0$ there, the given $k_- = \frac{1}{g}\left[h_- - \frac{3}{2}(gQ_-)^{2/3}\right]$. It follows from I(23) and Fig. I6 that $k_- > 0$, and that two values of F_-, one subcritical and one supercritical, are implied by the given $e_- = h_-$ and Q_-, as illustrated in Figs. 3-9. We can handle these two alternative incoming flows simultaneously. We shall use the fact that the solution of the jump conditions can be carried out as in §I5(c), and expressed in nondimensionalized form with respect to the incoming flow from the left as follows. The present version of I(78) is

$$F_- > \mu > 0 \quad \text{with} \quad \frac{\mu}{\lambda} = \frac{u_+}{(gd_-)^{1/2}}, \quad \lambda = \frac{d_+}{d_-} > 1 \tag{25}$$

from (21) and $(23)_2$. Then Theorem I17(ii) applies, as illustrated by Figs. I10(b) and (d), where

$$\mu = \lambda F_- - (\lambda - 1)\left[\frac{1}{2}\lambda(\lambda + 1)\right]^{1/2} \tag{26}$$

by I(73) and I(74) specialized to this type of normal transit. Each F_- value defines a unique λ_0 obtained by solving

$$F_- = \frac{\lambda_0 - 1}{\lambda_0}\left[\frac{1}{2}\lambda_0(\lambda_0+1)\right]^{1/2}, \tag{27}$$

which follows from $\mu = 0$ in (26). From I(48) and I(76) the bore speed is

$$-C = (gd_-)^{1/2}\left[\frac{1}{2}(\lambda(\lambda+1))^{1/2} - F_-\right]. \tag{28}$$

Theorem 2

(i) A bore which could relieve blocking as desired cannot exist if

$$\lambda_0 d_- \leq a .$$

(ii) A bore of the type (21) with (20) required to relieve blocking can exist upstream of the mountain if and only if

$$a < \lambda_0 d_- . \tag{29}$$

The strength λ of the bore lies within the ranges

$$\lambda_1 < \lambda_3 < \lambda_2 \leq \lambda < \lambda_0 \qquad \text{if} \quad F_- > 1 \ , \tag{30}$$

and

$$1 < \lambda_2 \leq \lambda < \lambda_0 \qquad \text{if} \quad F_- < 1 \ , \tag{31}$$

where $\lambda_1 = \frac{1}{2}\left[(1 + 8F_-^2)^{1/2} - 1\right]$ from I(83). Here λ_2 and λ_3 are defined in terms of a function $k_+(\lambda)$, which is monotonically increasing and convex in $\lambda_+ < \lambda < \lambda_0$, where

$$k_+(\lambda_+) = 0 \qquad \text{and} \qquad k_+(\lambda_0) = \lambda_0 d_- \ . \tag{32}$$

Fig. 10 illustrates $k_+(\lambda)$ and shows its juxtaposition with $\mu(\lambda)$ and $\lambda^{3/4}$. The value λ_2 solves

$$k_+(\lambda_2) = a \tag{33}$$

uniquely in the stated interval for each F_-. The values λ_3 and 1 solve

$$k_+(\lambda_3) = k_- \quad \text{if} \quad F_- > 1 \ , \qquad k_+(1) = k_- \quad \text{if} \quad F_- < 1 \ , \tag{34}$$

each uniquely within $\lambda_+ < \lambda < \lambda_0$.

(iii) In each range the outgoing velocity u_+ defined by (25) and (26) has $F_+ < 1$, i.e. the outgoing flow immediately to the right of the bore is subcritical regardless of whether the incoming flow is supercritical or subcritical. F_+ decreases as λ increases within the intervals (30) and (31).

(iv) Among the bores satisfying (30) and (31), the outgoing flow from the weakest one $\lambda = \lambda_2$ becomes critical and admits a bifurcation when it reaches the crest. In each case the corresponding least bore speed $-C = -(gd_-)^{1/2} B_-(\lambda_2)$ given by (28) is finitely separated from zero.

(v) Also among such bores, this weakest one involves the least energy dissipation E, and the least [e]. The stronger admissible bores travel faster and facilitate a free flow over the mountain which does not bifurcate.

(vi) Finally we give some properties of the pairs of flows designated by the presence and absence of an asterisk in I(19) - I(21). Here there exists a different such pair on each side of the bore, corresponding to h_-, Q_- upstream of it and h_+, Q_+ downstream. We show that

$$\left.\begin{aligned} & F_+ < F_-^* < 1 < F_- < F_+^* \\ \text{and} \quad & \\ & d_+^* d_-^* < d_+ d_- \end{aligned}\right\} \quad \text{if} \quad F_- > 1 \,, \tag{35}$$

$$\left.\begin{aligned} & F_+ < F_- < 1 < F_-^* < F_+^* \\ \text{and} \quad & \\ & d_+^* d_- < d_+ d_-^* \end{aligned}\right\} \quad \text{if} \quad F_- < 1 \,. \tag{36}$$

Proof

Application of the first part of Theorem I17(ii), with (25) and (26), identifies the admissible ranges

$$\lambda_1 < \lambda < \lambda_0 \quad \text{if} \quad F_- > 1, \quad \text{and} \quad 1 < \lambda < \lambda_0 \quad \text{if} \quad F_- < 1 \tag{37}$$

as illustrated in Figs. I10(b) and (d), since $\hat{F}_- = F_- > 0$ here. Theorem I17(ii) also implies $F_+ < 1$, which proves Theorem 2(iii) since $\hat{F}_+ = F_+ > 0$, because the admissible part of $\mu(\lambda)$ lies within $\mu^2 < \lambda^3$. Since $\mu(\lambda)$ is a decreasing function in the ranges (37), so is $F_+ = \mu(\lambda)/\lambda^{3/2}$.

The end points are excluded from (37) for the following reasons. The case $\lambda = \lambda_0$ requires $\mu = 0$, which is excluded by (25) because it would imply stagnant fluid on the right. The case $\lambda = \lambda_1$ when $F_- > 1$ is excluded because it would imply $C = 0$, which (21) does not allow because a hydraulic jump cannot relieve blocking. The case $\lambda = 1$ when $F_- < 1$ is excluded because there would be no change in depth and therefore no bore.

The definition $(20)_2$ of k_+ can be nondimensionalized, using $gQ_+ = gu_+d_+ = \mu(gd_-)^{3/2}$ from $(25)_2$, and $h_+ = \upsilon gd_-$ as shown after I(88), so that from $I(90)_1$ where $b = 0$

$$\frac{k_+}{d_-} = \frac{1}{2}\left[\frac{\mu}{\lambda}\right]^2 + \lambda - \frac{3}{2}\mu^{2/3} . \tag{38}$$

By (26) this defines a function $k_+(\lambda)$ for all $\lambda > 0$. Examples of $k_+(\lambda)$ for $F_- = 4$ and $F_- = 0.2$ are shown in Figs. 10(a) and (c). It is convenient, at first, to consider it on domains wider than (37). Theorem I16(iii) defines λ_+ to be the location of the intersection of $\lambda^{2/3}$ and $\mu(\lambda)$, so that $k(\lambda_+) = 0$ from (38). The value λ_0 satisfies $k_+(\lambda_0) = \lambda_0 d_-$, by putting $\mu = 0$ in (38), so proving (32). The gradient

$$\frac{1}{d_-}\frac{dk_+}{d\lambda} = 1 - \frac{\mu^2}{\lambda^3} - \left[1 - \left[\frac{\mu^2}{\lambda^3}\right]^{2/3}\right]\mu^{-1/2}\frac{d\mu}{d\lambda} .$$

Since $\mu < \lambda^{3/2}$ in $\lambda_+ < \lambda < \lambda_0$, which is wider than (37), $k_+(\lambda)$ is a monotonically increasing function satisfying $0 < k_+ < \lambda_0 d_-$ in that interval, and convex since $d^2k_+/d\lambda^2 > 0$, using $d\mu/d\lambda < 0$ which is assured a fortiori by Theorem I16(iii).

If $a \le k_+(\lambda)$ for some (not necessarily all) λ in either admissible range (37), it follows that $a < \lambda_0 d_-$. This proves sufficiency in (ii). Necessity follows by the contradiction between $a \ge \lambda_0 d_-$ and $a \le k_+ < \lambda_0 d_-$. This also proves (i).

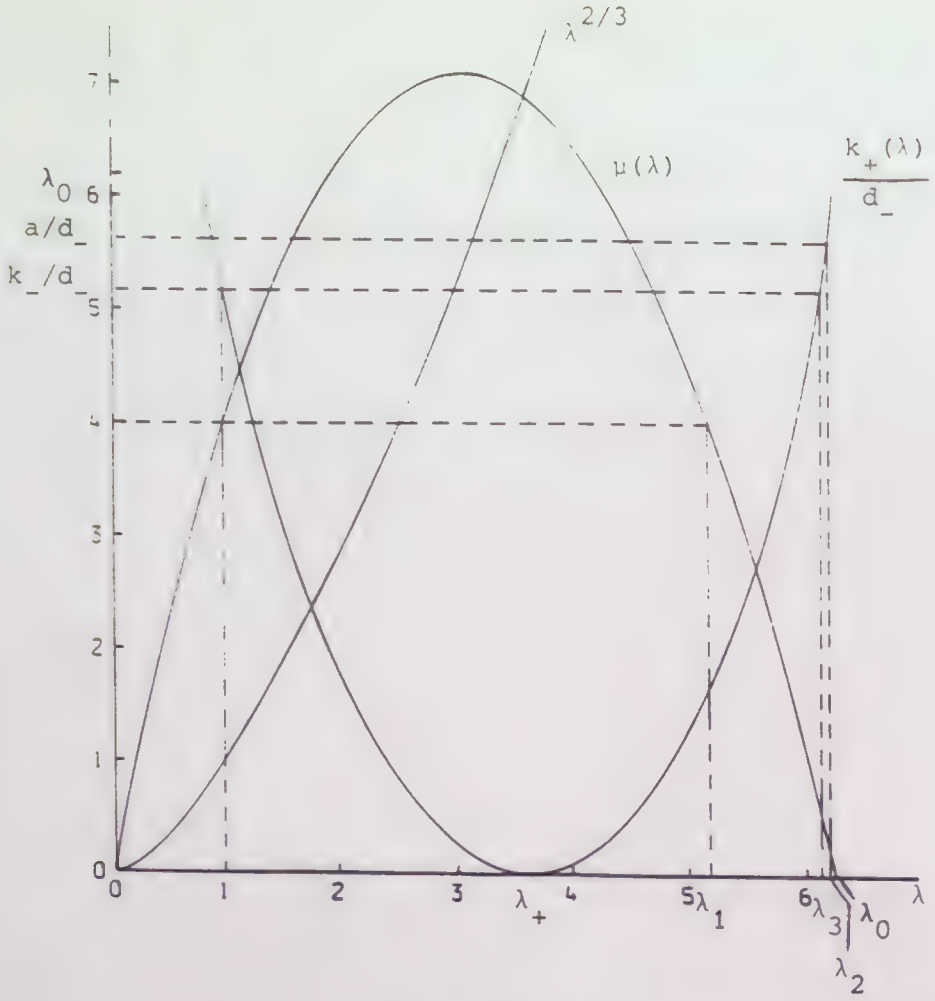

(a) $F_- = 4$

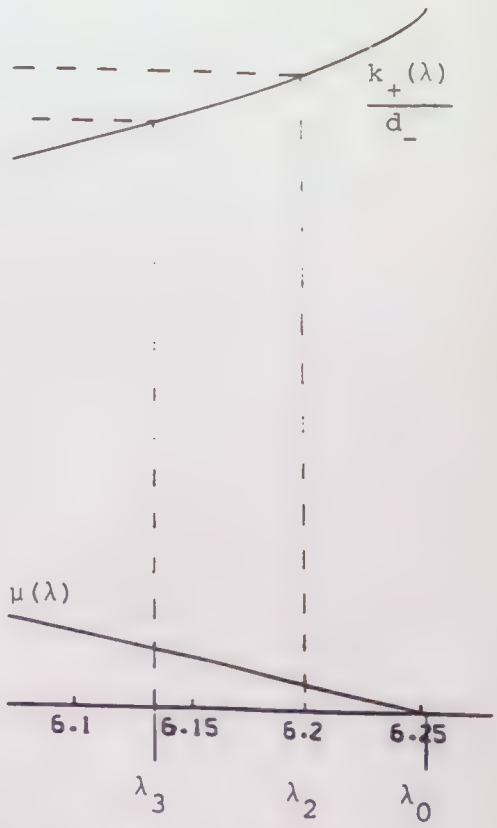

(b) $F_- = 4$ detail

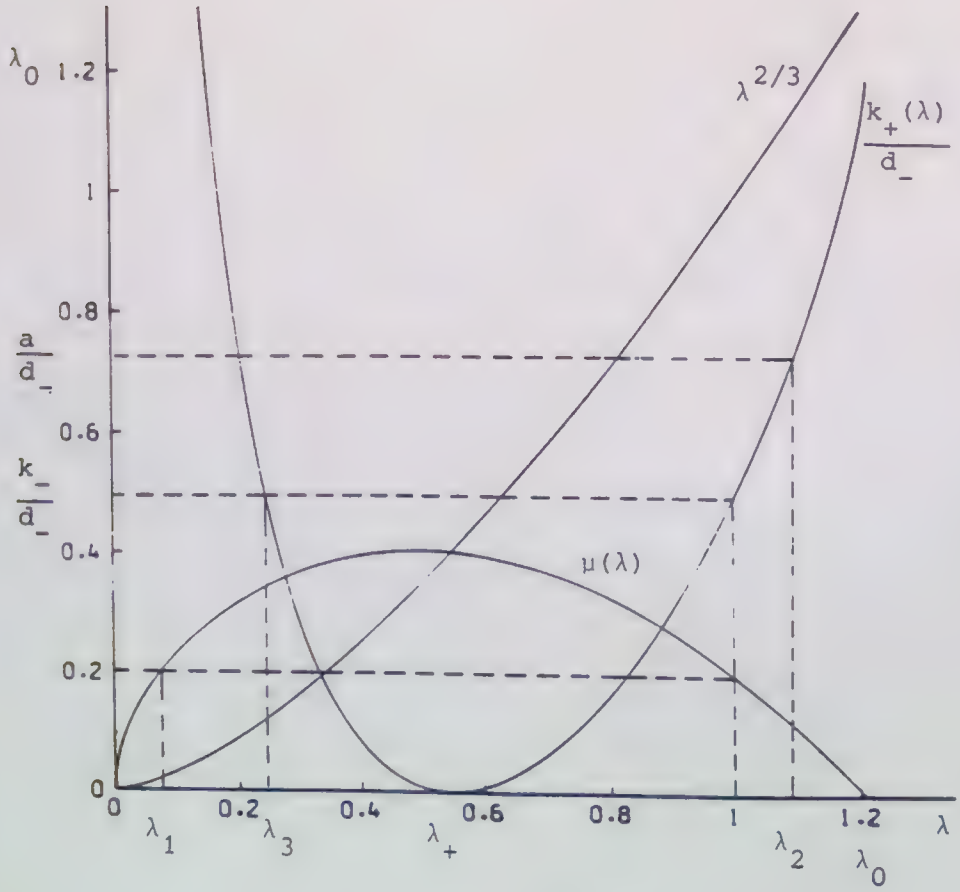

(c) $F_- = 0.2$

Fig. 10 The function $k_+(\lambda)$

As illustrated in Fig. 10, the monotonicity of $k_+(\lambda)$ proves that (33) defines λ_2 uniquely since $a < \lambda_0 d_-$. By the definitions $k_+(1) = k_-$ for all F_-, and λ_3 is the second root of $k_+(\lambda_3) = k_-$ as Fig. 10 shows. Since the range $\lambda_3 < \lambda_2 \leq \lambda < \lambda_0$ turns out to be rather small when $F_- = 4$, Fig. 10(b) shows an enlarged version of $k_+(\lambda)$ and $\mu(\lambda)$ within that range. When $F_- = 4$, $\lambda_1 = 5.18$. When $F_- < 1$, $\lambda_+ < 1$ from Theorem I16(iii) so that $1 < \lambda_2$ by the monotonicity because $k_- < a$. When $F_- > 1$, $\lambda_+ > 1$ so that $\lambda_3 < \lambda_2$ for the same reason. In this case it remains to prove $\lambda_1 < \lambda_3$, which also follows from the monotonicity because

$$k_+(\lambda_1) - k_- = -\frac{(\lambda_1 - 1)^3}{4\lambda_1} d_- < 0 .$$

This completes the proof of (ii).

The minimizing property of E follows from the monotonic character of $I(89)_1$.

Since $[e] = [h]$ and $h_+ = \upsilon g d_-$, the minimizing property of e_+ and $[e]$ is equivalent to that of υ. Since Fig. I3 also expresses I(87), the minimizing property of $\upsilon(\lambda)$ at λ_2 is seen to follow by lifting the decreasing curve $\mu(\lambda)$ onto the subcritical part of the surface. Equivalently, the fact that $\upsilon(\lambda)$ is an increasing function can be established analytically, but at greater length.

The final two properties in (v) follow from the monotonicity of $B_-(\lambda)$ in (28), illustrated in Fig. I10(b) and (d), and of $k_+(\lambda)$.

To prove (vi), note that for $F_- > 1$ and a bore of strength λ_3 I(23), $(23)_1$ and $(34)_1$ imply $G_+ > G_-$, where G is the constitutive function defined by I(22). Reference to Fig. I6 shows that $F_+ < F_-^* < 1 < F_- < F_+^*$ for such a bore and therefore for all bores satisfying (30), by the monotonicity of F_+.

For bores satisfying (31), $F_+ = \mu(\lambda)/\lambda^{3/2} < F_-$ and therefore $F_+ < F_- < 1 < F_-^* < F_+^*$, by referring to Fig. I6 again.

The inequalities involving $d_\pm$, $d_\pm^*$ now follow from $I(20)_1$, because $\frac{1}{4} F [(8 + F^2)^{1/2} + F]$ is an increasing function of $F > 0$. □

We illustrate Theorem 2 with symmetric parabolic and quartic obstacle profiles. These are

$$b(x) = a\left[1 - \left[\frac{x}{\ell}\right]^2\right] \qquad \text{and} \qquad b(x) = a\left[1 - \left[\frac{x}{\ell}\right]^4\right] \tag{39}$$

for $|x| \leq \ell$, respectively, with $b(x) = 0$ elsewhere. The former admits an abrupt bifurcation of the free surface profile above the top, like that in Fig. 9. The quartic obstacle with $\sigma = 4$, $\nu = 0$ in (6) admits a smooth bifurcation of the horizontal free surface above the top, like Figs. 7 and 8.

We show the two examples in Figs. 11 and 12. In each case we choose $g = 1$ with $Q_- = 9$ and $e_- = 7.5$ so that, as in Figs. 3-9, there are two incoming flows on the flat plain to the left of the mountain with

$$\begin{aligned} F_- &= 0.54\ , \qquad u_- = 1.37\ , \qquad d_- = 6.56\ , \\ F_- &= 1.73\ , \qquad u_- = 3\ , \qquad\ \ d_- = 3\ . \end{aligned} \tag{40}$$

Such pairs of values satisfy I(20) and I(21), and are consistent with Fig. I6. We have $k_- = 1.01$ from (19), and we choose $a = 1.2$ so that these incoming flows are blocked, and could only progress as far as the end of the contour shown by short dashes in Figs. 11 and 12, after which this γ contour would have to turn back like contour 7 in Figs. 3-9.

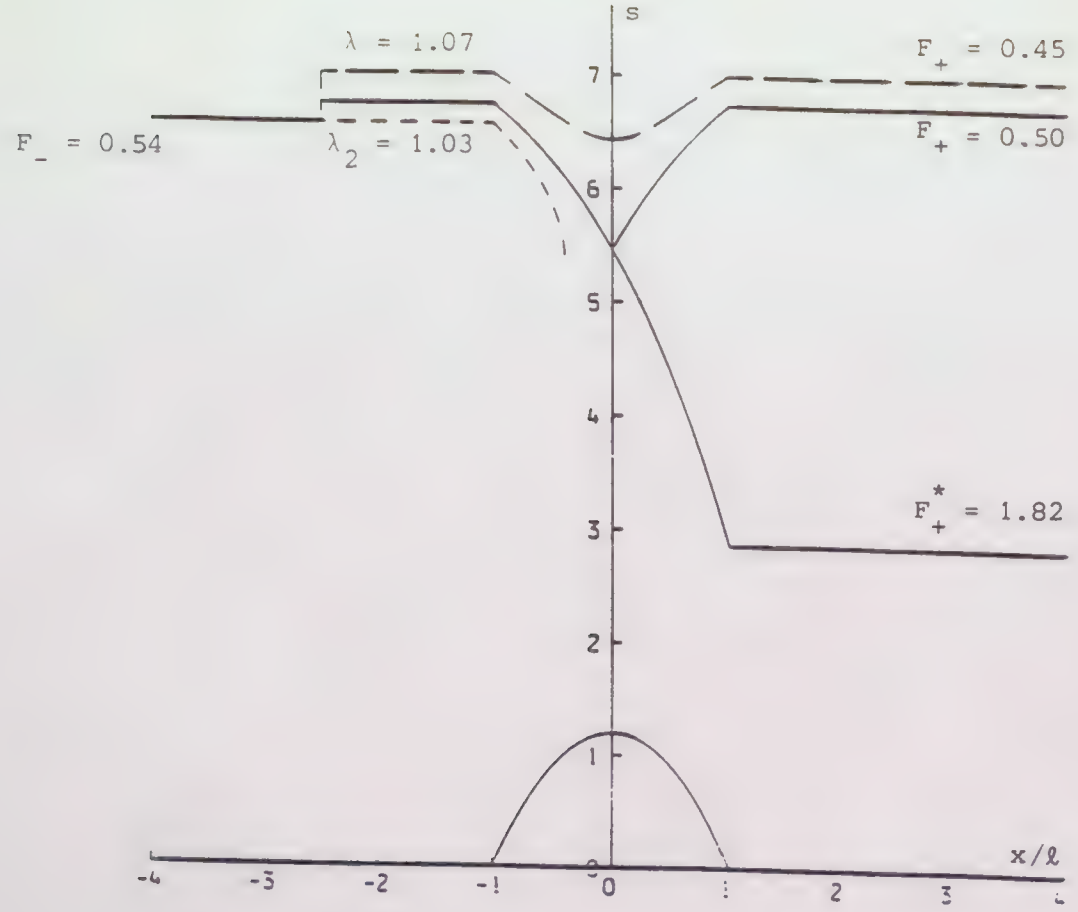

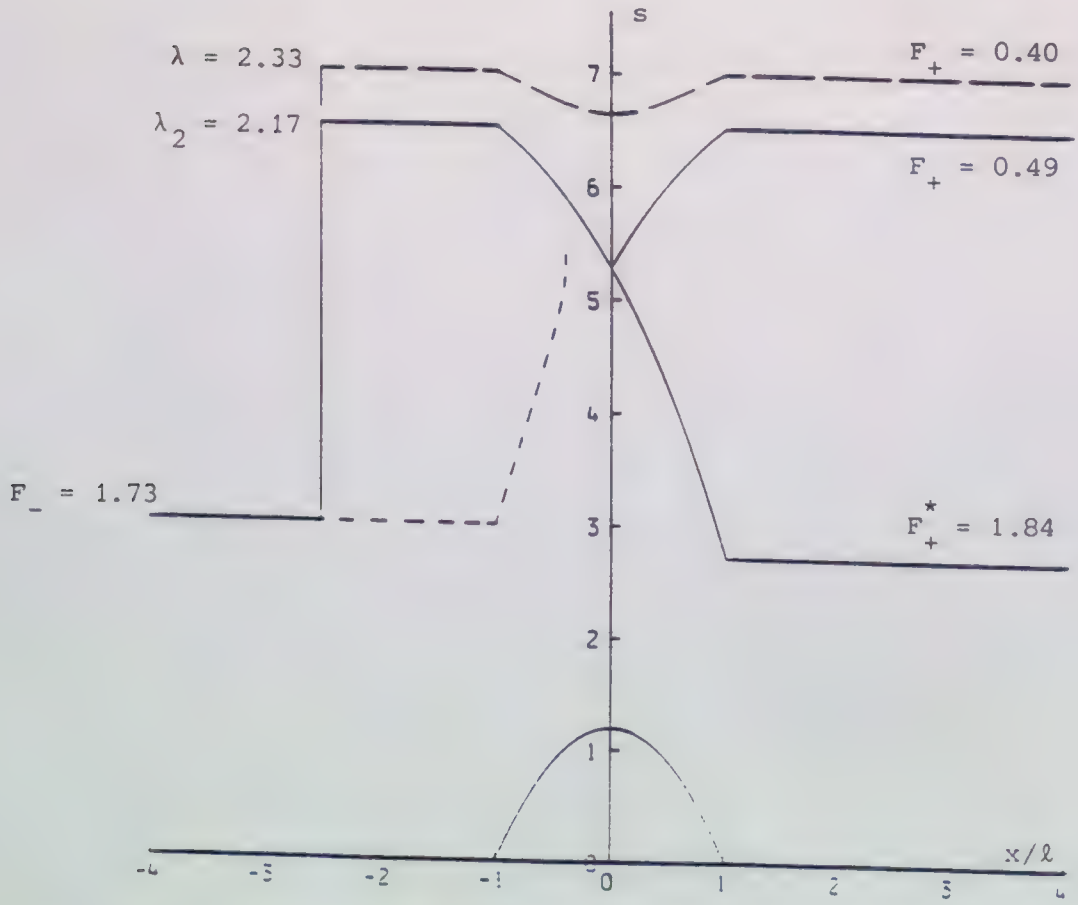

Fig. 11 Relief of blocking over a symmetric parabolic mountain.

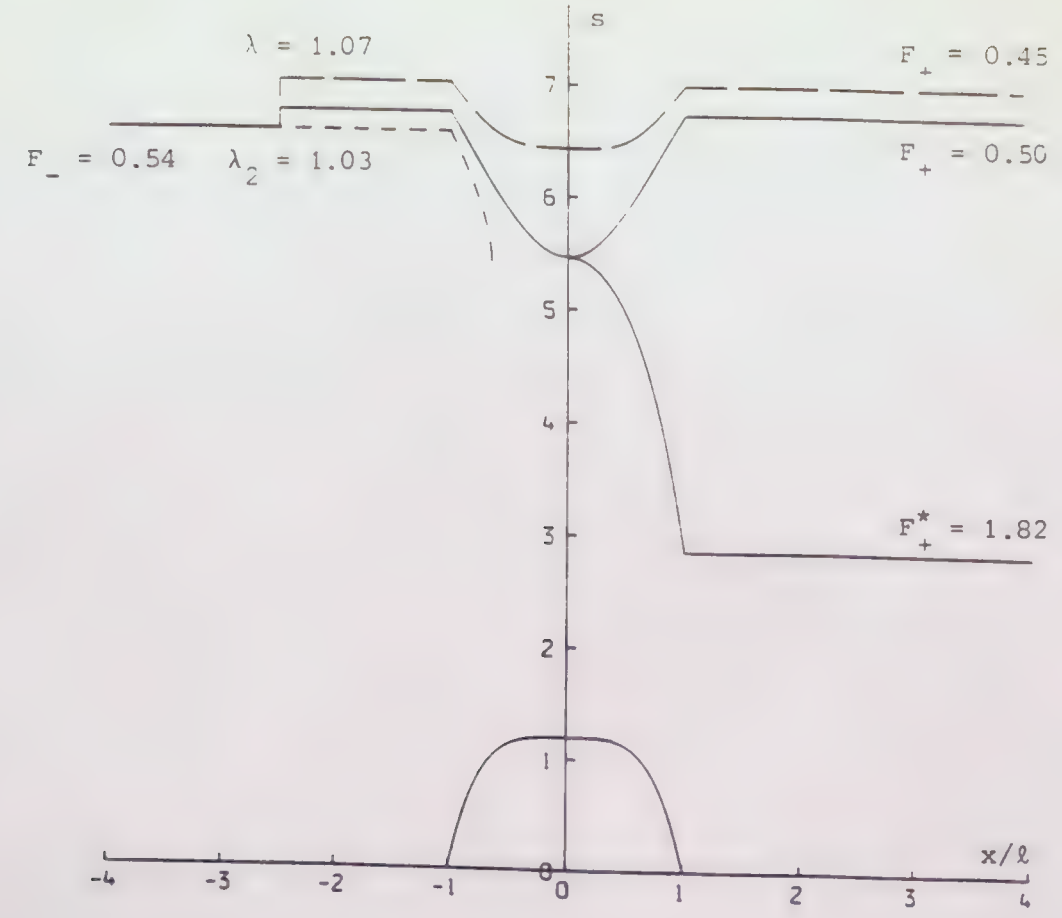

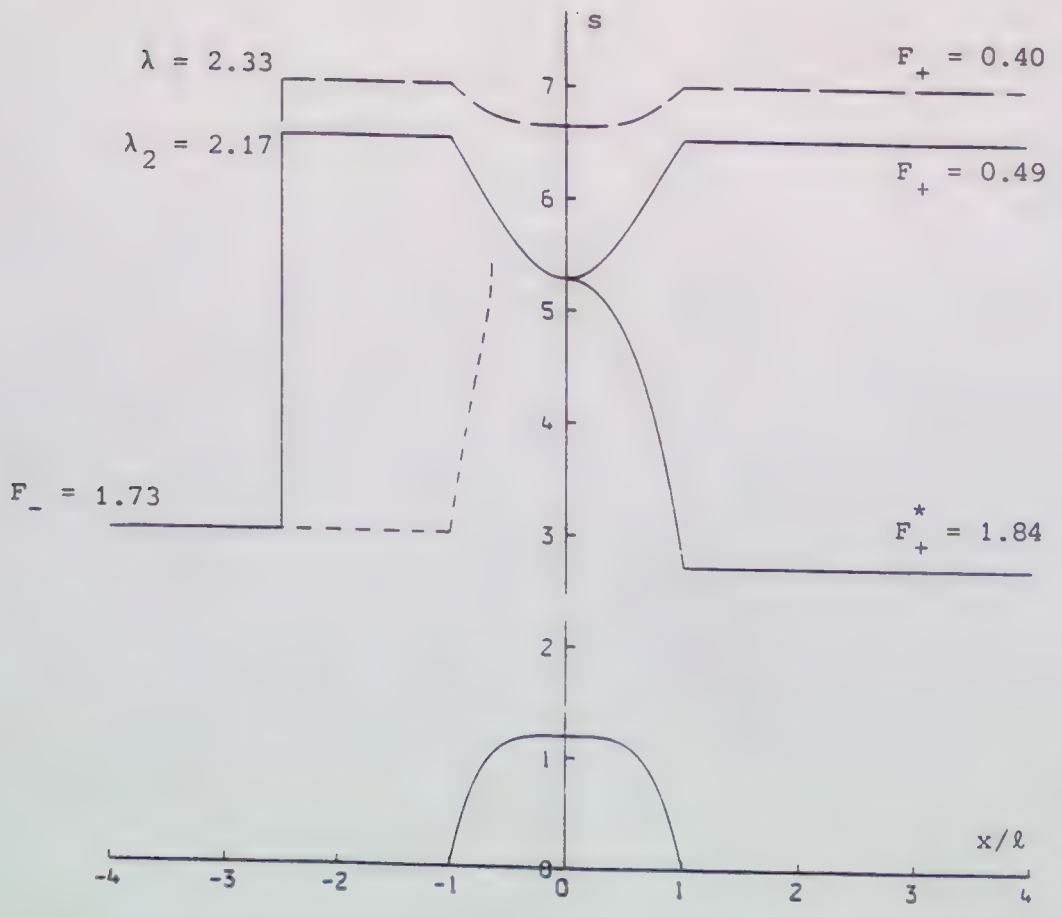

Fig. 12 Relief of blocking over a symmetric quartic mountain.

The block can be overcome by a bore travelling to the left over the flat plain, and we show two such bores on each diagram in Figs. 11 and 12. These Figures illustrate the various general properties proved in Theorem 2.

The full line shows a bore which overcomes the block with minimum energy dissipation $E(\lambda_2)$ in I(89), so that the outgoing flow can branch at the top according to Theorem 2(iv). Thus we have $k_+ = a = 1.2$ for the outgoing flow to the right of the bore. The diagrams show how the free surface branches over the top, abruptly for the semi-circle and smoothly for the quartic. For the subcritical incoming flow we find that the bore has minimum strength $\lambda_2 = 1.03$ and the immediately outgoing subcritical flow has

$$F_+ = 0.50 , \qquad u_+ = 1.30 , \qquad d_+ = 6.73 . \tag{41}$$

These values (41) are recoverable, after the bifurcation, downstream on the flat plain to the right of the mountain. The bifurcation also makes available a supercritical flow to the right of the top, and when this reaches the flat plain downstream it has

$$F_+^* = 1.82 , \qquad u_+^* = 3.08 , \qquad d_+^* = 2.86 . \tag{42}$$

For the supercritical incoming flow, the minimum bore strength $\lambda_2 = 2.17$ and the immediately outgoing subcritical flow has

$$F_+ = 0.49 , \qquad u_+ = 1.26 , \qquad d_+ = 6.52 . \tag{43}$$

These values also are recoverable, after the bifurcation, downstream of

the mountain. The bifurcation also makes available a supercritical flow to the right of the top having

$$F_+^* = 1.84 \ , \qquad u_+^* = 3.03 \ , \qquad d_+^* = 2.72 \tag{44}$$

downstream of the mountain.

The curves shown by long dashes in Figs. 11 and 12 illustrate how a bifurcation is avoided if the bore dissipates more energy than the minimum value $E(\lambda_2)$. If λ lies strictly within the ranges (30) and (31), the outgoing flow to the right of the bore is a free flow past the top for arbitrarily small $\lambda - \lambda_2$, which does not bifurcate. To achieve a clear diagram, however, in the case of the subcritical incoming flow we have chosen a bore of strength $\lambda = 1.07 > \lambda_2 = 1.03$ with $k_+ = 1.52 > a = 1.2$, and

$$F_+ = 0.45 \ , \qquad u_+ = 1.2 \ , \qquad d_+ = 7 \tag{45}$$

on the flat plain downstream of the bore. For the supercritical incoming flow we have chosen a bore of strength $\lambda = 2.33 > \lambda_2 = 2.17$ with $k_+ = 1.88 > a = 1.2$, and

$$F_+ = 0.40 \ , \qquad u_+ = 1.05 \ , \qquad d_+ = 7 \tag{46}$$

on the flat plain downstream of the bore.

The bores are shown when they are in the same place, for convenience, but they will be moving at different speeds to the left, as given by Figs. I10(b) and (d). The speeds of the weakest bore, from (28), are

$$- C(\lambda_2) = 1.24 \quad \text{and} \quad 0.22 \tag{47}$$

when it meets subcritical and supercritical incoming flow, respectively, in Figs. 11 and 12, and those of the stronger bore are

$$-C(\lambda) = 1.32 \quad \text{and} \quad 0.42 \ . \tag{48}$$

Bores which meet the subcritical flow are evidently much faster than those which meet the supercritical flow.

Next we examine how the range of admissible bores described in Theorem 2(ii) depends on the incoming flow. On the flat plain to the left of the mountain we have, from the general formula I(23),

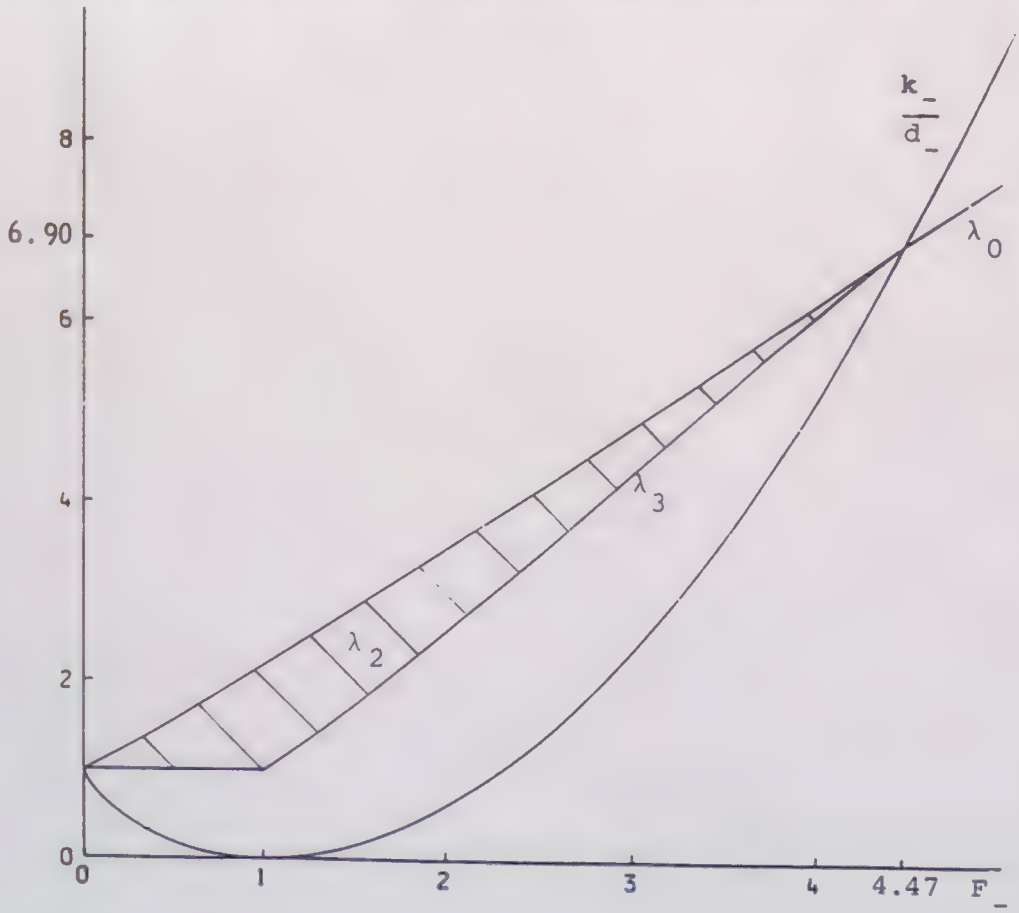

Fig. 13 Limit of blocking at the intersection of λ_0, λ_3 and k_-/d_- as functions of F_-.

$$\frac{k_-}{d_-} = \frac{1}{2} F_-^2 + 1 - \frac{3}{2} F_-^{2/3} \qquad (49)$$

for any steady incoming flow. This function is shown in Fig. 13. Also shown there is the function $\lambda_0(F_-)$ which is the unique inverse of (27).

Theorem 3

Blocking cannot be relieved if $F_- > 4.47$, and no bore which relieves blocking has strength greater than 6.90.

Proof

The values specified in the Theorem are those corresponding to the intersection of the functions (49) and $\lambda_0(F_-)$ in Fig. 13. It can be seen by examining the ordinates in Fig. 10 that the stated intersection is where the ranges of admissible λ in (30) and (31) are reduced to zero, i.e. $k_-/d_- = \lambda_0 = 6.90$ there. □

The result can be confirmed in another way by examining the abscissae in Fig. 10, i.e. by plotting the function $\lambda_3(F_-)$ in Fig. 13 and observing that it passes through the same intersection point. The definition of λ_3 via $k_+(\lambda_3) = k_-$ as in (34) is

$$\frac{1}{2}\left[\frac{\mu(\lambda_3)}{\lambda_3}\right]^2 + \lambda_3 - \frac{3}{2}\mu(\lambda_3)^{2/3} = \frac{1}{2} F_-^2 + 1 - \frac{3}{2} F_-^{2/3}$$

for all $F_- > 0$, where F_- is present as a parameter on the left also, by (26). The function $\lambda_1(F_-)$ always lies below $\lambda_0(F_-)$.

For each given F_- the admissible values of λ_2 must lie within the hatched region shown in Fig. 13, and the corresponding admissible

mountain top heights a for which blocking is relievable lie between the two curves $k_-/d_- < a/d_- < \lambda_0$ as we have seen.

The solutions described in this Section involve a bore upstream of the mountain, and travelling in the upstream direction, to the left. The flow to the right of the bore, whether it be free, or branched at the top, is steady. The flow to the left of the bore is steady except for the moment when the bore arrives, when it undergoes the associated discontinuities. For this reason it is accurate to call the overall flow pseudo-steady. When the bore is over the mountain the flow to the right of it will not be steady, as is well recognised at least for free flows there.

Our concern has been to give a thorough account of <u>local</u> conditions, and this has revealed, in particular, the availability of a smooth bifurcation at the top of certain obstacles which we have not seen reported elsewhere. In so far as conditions at a far distance downstream will choose between the two flows thus made available at the top, the range of possible types of such conditions is thereby widened by our solutions.

4. <u>Hydraulic Jump in a Free or Branched Flow</u>

In this Section we examine the types of hydraulic jump which can occur in a regime of steady one dimensional flow in the direction of the positive x axis, without the supposition that the flow is blocked by a mountain.

As in Theorem 1, the incoming flow from the left will have constants $Q > 0$ and e_-, by (2), and the outgoing flow will have constants Q and e_+, where $e_+ < e_-$ from I(61). The jump will have the swallowtail property shown in Fig. I7 but in h,Q,P space, by the remark after

Theorem I9. From I(51) and I(52) we have $0 < u_+ < u_-$ and $d_+ > d_-$, so that I(65) holds and the jump has the profile of Fig. I9. That is, a jump cannot face downstream, but only upstream. The strength of the jump is

$$\lambda = \frac{d_+}{d_-} = \frac{u_-}{u_+} .$$

The jump may exist at any location with local bed height b, either non-zero over an obstacle or zero over a flat plain.

Now suppose that the incoming flow would be branched with respect to some top height a to the right of the jump, i.e. that

$$k_- = a \qquad \text{where} \qquad k_- = \frac{1}{g}\left[e_- - \frac{3}{2}(gQ)^{2/3}\right] .$$

Then the immediately outgoing flow must satisfy

$$k_+ < a \qquad \text{where} \qquad k_+ = \frac{1}{g}\left[e_+ - \frac{3}{2}(gQ)^{2/3}\right]$$

and would therefore be blocked. It follows that if a hydraulic jump of this type were situated to the left of the mountain, a bore of the type described in §3 would need to intervene over the flat plain between the jump and the mountain in order to relieve the blocking, by the mechanism described in §3.

Next assume that the incoming flow would be free in the sense that $k_- > a$. Then since

$$k_+ - a = \frac{E}{gQ} + k_- - a$$

from I(55) and I(61), the outgoing flow will be free, branched or blocked according to whether the energy dissipated at the jump satisfies

$$-\frac{E}{gQ} < , = , > k_- - a \qquad (50)$$

respectively, i.e. depending on how $k_- - a$ is related to the strength of the jump via I(89).

5. Bore in a Free or Branched Flow

As with a hydraulic jump, there is no reason in principle why a bore should not be present in a pseudo-steady flow, even when the bore is not needed to relieve blocking.

Here we examine such bores, when there is a steady incoming flow from the left with constants $Q_- > 0$ and e_-, and associated

$$k_- = \frac{1}{g}\left[e_- - \frac{3}{2}(gQ_-)^{2/3}\right]$$

from (19). We assume $k_- > 0$, so that where the flow is over a flat plain $b = 0$ it may be subcritical or supercritical by Fig. I6. We also assume that $k_- \geq a$, so that the flow would not be blocked by an apex height $a > 0$ to the right of the bore.

We consider a bore which is travelling to the left, and which allows the direction of motion of the particle to be sustained after they meet. In addition we assume that the flow immediately to the right of the bore is a steady continuous one with constants $Q_+ > 0$ and e_+ with associated k_+ satisfying (20). This is the same type of bore as was considered in §3.

Theorem 4

Suppose that

$$k_- = a < \lambda_0 d_- \ . \tag{51}$$

Then the incoming flow, whether it be subcritical or supercritical, could travel continuously to the top and bifurcate there.

In addition, the flow could meet an upstream bore of the kind just described, to the left of the mountain, whose strength λ satisfies Theorem 2 except that

$$\lambda_2 = \lambda_3 \quad \text{if} \quad F_- > 1 \ , \qquad \lambda_2 = 1 \quad \text{if} \quad F_- < 1 \ . \tag{52}$$

If $k_+ = a$, minimum energy is dissipated at the bore, which has minimum strength λ_3 if $F_- > 1$, and unity (implying no bore) if $F_- < 1$. For $F_- > 1$, the outgoing flow from the bore will be subcritical with F_+ less than the associated incoming $F_-^* < 1$, and this outgoing flow also bifurcates at the top of the mountain. The free surface height at such a bifurcation point is less than if the bore had not intervened, and decreases as λ_3 increases.

If $k_+ > a$, more energy than the minimum is dissipated, the minimum bore strength is exceeded, and the outgoing flow is a free subcritical one, for both subcritical and supercritical incoming flow.

Proof

The conclusion (52) can be read off the representative situation in Fig. 10, i.e. when the ordinates a/d_- and k_-/d_- coincide, so do the corresponding ascissae λ_2 and λ_3, or λ_3 and 1.

Theorem 2 as thus amended tells us that the weakest admissible bore

has strength λ_3 if $F_- > 1$ and facilitates a subsequent bifurcation, and that stronger bores induce a free flow; but if $F_- < 1$ the weakest admissible $\lambda = 1$ which is not in fact a bore, and only the stronger admissible $\lambda > 1$ define a bore, which then induce a free flow.

From I(23)

$$G = \frac{2g(k-b)}{3(gQ)^{2/3}} + 1 \ . \tag{53}$$

The right side increases across a bore having $k_- = a = k_+$ since $Q_+ < Q_-$ there by (23), so that $G_+ > G_-$. Fig. I6 shows that $G(F)$ is a convex function of F with stationary minimum at $F = 1$, and therefore the subcritical outgoing F_+ is less than the subcritical incoming F_-.

The free surface height over the top at any bifurcation point is

$$\frac{2e}{3g} - \frac{1}{3}a = \frac{(gQ)^{2/3}}{g} + a$$

since $F = 1$ there, in terms of the constants e and Q of the associated continuous flow. By $Q_+ < Q_-$ this decreases if a bore intervenes. The height without a bore exceeds the height with a bore by

$$\frac{1}{g}\left[(gQ_-)^{2/3} - (gQ_+)^{2/3}\right] = d_-\left[F_-^{2/3} - \mu^{2/3}\right]$$

in which μ is a function of λ_3 which decreases as λ_3 increases. □

Fig. 14 shows an example in which <u>two</u> different bifurcations at the top are available to an incoming flow, as justified by Theorem 4. The mountain (6) is a symmetric ($\upsilon = 0$) cubic ($\sigma = 3$) one, and each incoming flow from the left has $Q_- = 9$, $e_- = 7.5$ with $g = 1$. Then

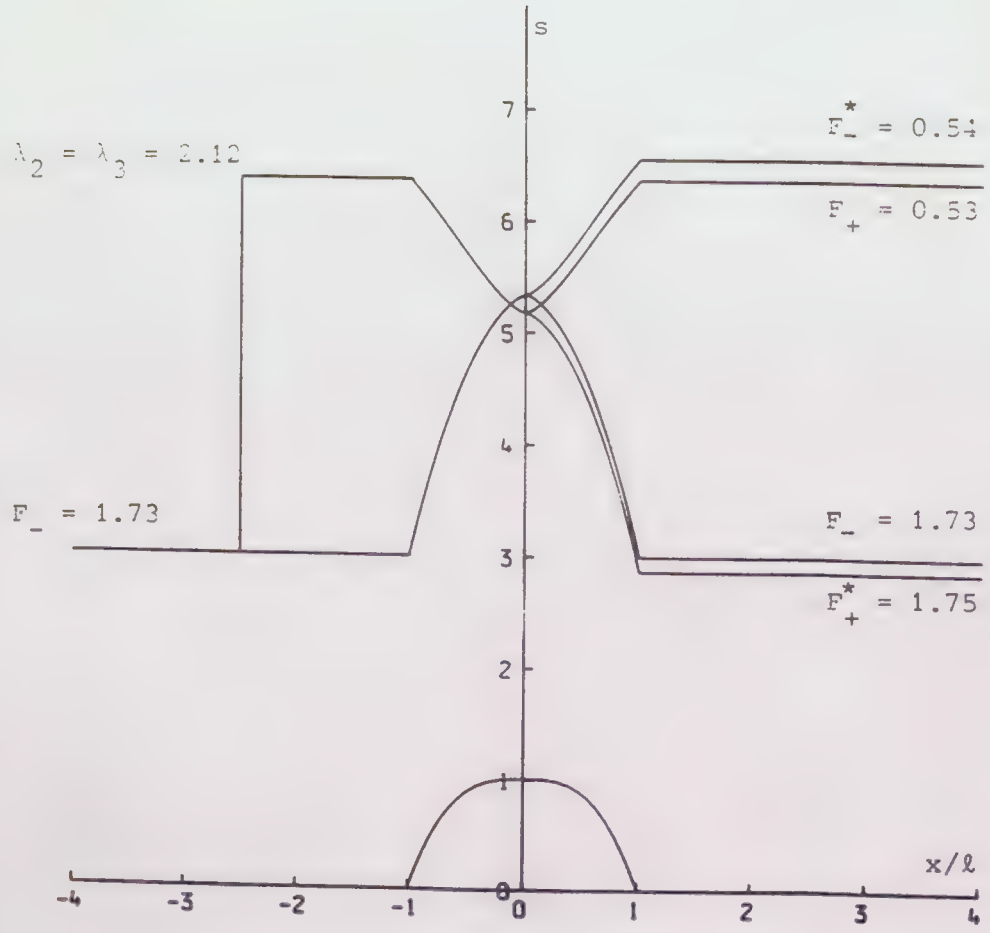

Fig. 14 Two bifurcations available to a supercritical flow

$k_- = 1.01 = a$, so that both the subcritical and supercritical incoming flows attain the same bifurcation point at the top (cf. contour 6 in Fig. 7). The free surface diagram of Fig. 14 shows only the supercritical incoming flow. Over the flat plain this has $u_- = s_- = 3$ and $F_- = 1.73$. If the bore does not intervene the bifurcation point is the higher one shown in Fig. 14. According to Theorem 4, however, a bore of minimum strength 2.12 given by $(52)_1$ can intervene before the mountain, such that $Q_+ = 8.49$ and $k_+ = k_-$. The bore travels to the left with speed 0.15, and induces a subcritical flow to its right with depth 6.36. When this flow reaches the apex it has available to it the lower bifurcation point shown in Fig. 14, after which the flow may be

subcritical again, or supercritical with eventual depth 2.86, which is less than the incoming one.

Theorem 5

Suppose that

$$a < \min (k_-, \lambda_0 d_-) \ . \tag{54}$$

Then the incoming flow, whether it be subcritical or supercritical, is a free flow.

In addition, the flow could meet an upstream bore of the kind described at the beginning of this Section, to the left of the mountain, whose strength satisfies

$$\max (\lambda_1, \lambda_2) \leq \lambda < \lambda_0 \qquad \text{if} \qquad F_- > 1 \tag{55}$$

and

$$1 < \lambda < \lambda_0 \qquad \text{if} \qquad F_- < 1 \ . \tag{56}$$

If $\lambda_1 \geq \lambda_2$ a hydraulic jump is also admissible in (55), with $\lambda = \lambda_1$.

As in Theorem 2(iii) the immediately outgoing flow is subcritical.

The outgoing flow may either be free or,

$$\text{if} \quad \lambda_2 \geq \lambda_1 \quad \text{when} \quad F_- > 1 \ , \tag{57}$$

it may admit a bifurcation at the top of the mountain.

The outgoing flow will be free, and cannot admit a bifurcation,

$$\text{when} \quad F_- < 1 \ , \qquad \text{or if} \quad \lambda_2 < \lambda_1 \quad \text{when} \quad F_- > 1 \ . \tag{58}$$

Proof

Hypothesis (54) is sufficient for $k_- > a$, which is the defining property of a free flow.

From Theorem I17(ii) we deduce that the immediately outgoing flow from the bore must be subcritical, as in Theorem 2(iii), and we obtain the admissible ranges

$$\lambda_1 \leq \lambda < \lambda_0 \quad \text{if} \quad F_- > 1 , \quad \text{and} \quad 1 < \lambda < \lambda_0 \quad \text{if} \quad F_- < 1 \qquad (59)$$

in place of (37). Here we can admit a hydraulic jump $\lambda = \lambda_1$ when $F_- > 1$ since we are not now seeking to relieve blocking (cf. Theorem 1).

The convex function $k_+(\lambda)$ defined by (38) is again available and is monotonically increasing in the ranges (59), as illustrated in Fig. 10.

Examination of Fig. 10 is enough to indicate that λ_3 is now irrelevant because $k_- > a$ so that $\lambda_3 > \lambda_2$. When $F_- < 1$, $k_- > a$ implies $1 > \lambda_2$, and $(59)_2$ confirms (56) as Fig. 10(c) illustrates. When $F_- > 1$ Fig. 10(a) shows that the whole interval $(59)_1$ is available if $\lambda_2 \leq \lambda_1$, and that only the part (55) of it is available if $\lambda_2 > \lambda_1$.

The outgoing flow is a free flow if $k_+(\lambda) > a$, i.e. if $\lambda > \lambda_2$, and a branched flow if $k_+(\lambda) = a$, i.e. if $\lambda = \lambda_2$. The latter is available in (55) when (57) applies. The property $k_+(\lambda_0) = \lambda_0 d_-$ of the monotonic $k_+(\lambda)$ shows that the hypothesis $a < \lambda_0 d_-$ in (54) is necessary to ensure that the outgoing flow shall not be blocked. □

The hydraulic jump of strength λ_1 which Theorem 5 admits for supercritical incoming flow gives a situation in which <u>two steady</u> flows are possible, namely one free flow without the jump, and one flow with

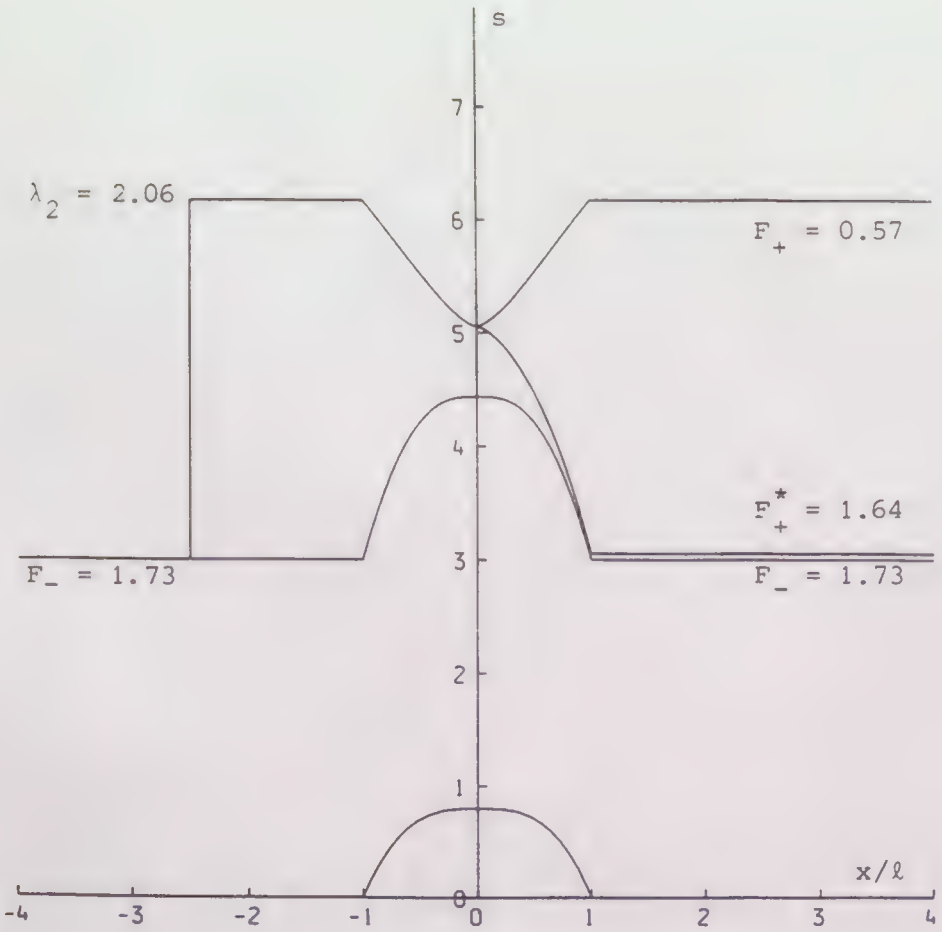

Fig. 15 One bifurcation available to a supercritical free flow

the jump. The latter is a free flow

$$\text{if} \quad \lambda_1 > \lambda_2 \quad \text{and has} \quad k_- - a > -\frac{E(\lambda_1)}{gQ}$$

from (50), and is a branched flow

$$\text{if} \quad \lambda_1 = \lambda_2 \quad \text{and has} \quad k_- - a = -\frac{E(\lambda_2)}{gQ} \, .$$

By contrast, a flow with a bore is only pseudo-steady.

Fig. 15 shows an example in which an incoming supercritical free flow can be converted to a flow having a bifurcation at the top, by the intervention of a bore moving to the left, as justified by (57) in

Theorem 5. Again the mountain (6) is a symmetric ($\upsilon = 0$) cubic ($\sigma = 3$) one, and each incoming flow from the left has $Q_- = 9$, $e_- = 7.5$ with $g = 1$. Thus $k_- = 1.01$ as before, but now the apex height is $a = 0.8$. The free surface of the supercritical free flow over the mountain is shown in Fig. 15 (cf. contour 5 in Fig. 7). Over the flat plain this has $u_- = d_- = 3$ and $F_- = 1.73$. The bore which it meets has strength $\lambda_2 = 2.06$ determined from $k_+(\lambda_2) = 0.8$ in (38), so that the new flow has depth $d_+ = 6.17$ on either side of the mountain. Then $u_+ = 1.42$ and $F_+ = 0.57$ there from (25), so that the constants of the new flow are $Q_+ = 8.78$ and $e_+ = 7.18$. The bore speed to the left is 0.07. The new supercritical flow which emerges from the bifurcation eventually has depth 3.05, speed 2.87 and Froude number 1.64 on the right of the obstacle.

6. Summary of Solutions

Fig. 16 summarizes some of the features of the steady and pseudo-steady solutions found in this paper. It is expressed in terms of the Froude number F_- of the incoming flow, and the ratio a/d_- of the mountain apex height to the flow depth, over the flat plain on the upstream side, of that incoming flow. This enables one to compare our results directly with those of the authors mentioned in the Introduction.

Curve A expresses the condition $k_- = a$ for the incoming flow to be a branched flow. From (49) the condition that an incoming flow over the flat plain shall branch at the top can be written

$$\frac{a}{d_-} = \frac{1}{2} F_-^2 + 1 - \frac{3}{2} F_-^{2/3} . \qquad (60)$$

This is curve A. Any point above it in Fig. 16 represents a blocked

flow, and any point below it represents a continuous free flow. The latter may be either subcritical or supercritical or (only when $a < 0$) critical.

Curve B expresses the condition $\lambda_0 d_- = a$ or $k_+(\lambda_0) = a$ or $\lambda_0 = \lambda_2$. We have seen in Fig. 13 that the relation (27) between F_- and the strength λ_0 of that bore which reduces the immediately outgoing flow on its right to rest is single valued. Curve B is therefore

$$F_- = \frac{a - d_-}{a}\left[\frac{a}{2d_-}\left[\frac{a}{d_-} + 1\right]\right]^{1/2} . \qquad (61)$$

Points on this curve represent cases where the depth $\lambda_0 d_-$ of the <u>incipient</u> outgoing flow (from the bore off the mountain) is equal to the mountain apex height. In other words, curve B represents cases where there is a stagnant reservoir whose depth is the height of the mountain bounding it on the right, and whose boundary on the left is a bore moving to the left with speed

$$(gd_-)^{1/2}\left[\frac{a + d_-}{2a}\right]^{1/2}$$

from (28) and (61). This speed is just enough to reduce the fluid which crosses the bore to rest at a rate which sustains the top of the reservoir at the mountain top level.

The unique intersection point of curves A and B is at $F_- = 4.47$ and $a/d_- = 6.90$. Blocking (when it exists) is unrelievable at higher values.

Curve C represents the condition that a supercritical incoming free flow can encounter, upstream of the mountain, a hydraulic jump which

is capable of converting it to a subcritical branched flow. Theorem 5 justifies this possibility. A hydraulic jump has strength

$$\lambda_1 = \frac{1}{2}\left[(1 + 8\,F_-^2\,)^{1/2} - 1\right]$$

from I(83), and satisfies $Q_+ = Q_-$ so that the Froude number of the immediately outgoing flow is

$$F_+ = \lambda_1^{-3/2}\,F_- \,.$$

This outgoing flow branches at the apex if $k_+ = a$, i.e. if

$$\frac{a}{d_+} = \frac{1}{2}F_+^2 + 1 - \frac{3}{2}F_+^{3/2}$$

immediately to the right of the jump. Eliminating F_+ and λ_1 from these last three equations gives the relation

$$\frac{a}{d_-} = \frac{1 + (1 + 8F_-^2)^{3/2}}{16F_-^2} - \frac{3}{2}F_-^{3/2} - \frac{1}{4} \qquad (62)$$

describing curve C in Fig. 16.

Points on curve C have the property $\lambda_1 = \lambda_2$. This can be verified by expressing it as $k_+(\lambda_1) = k_+(\lambda_2) = a$, using the monotonicity of $k_+(\lambda)$ in (38), and the definition of λ_2. Then since $\mu(\lambda_1) = F_-$ from Theorem I16(ii) we have

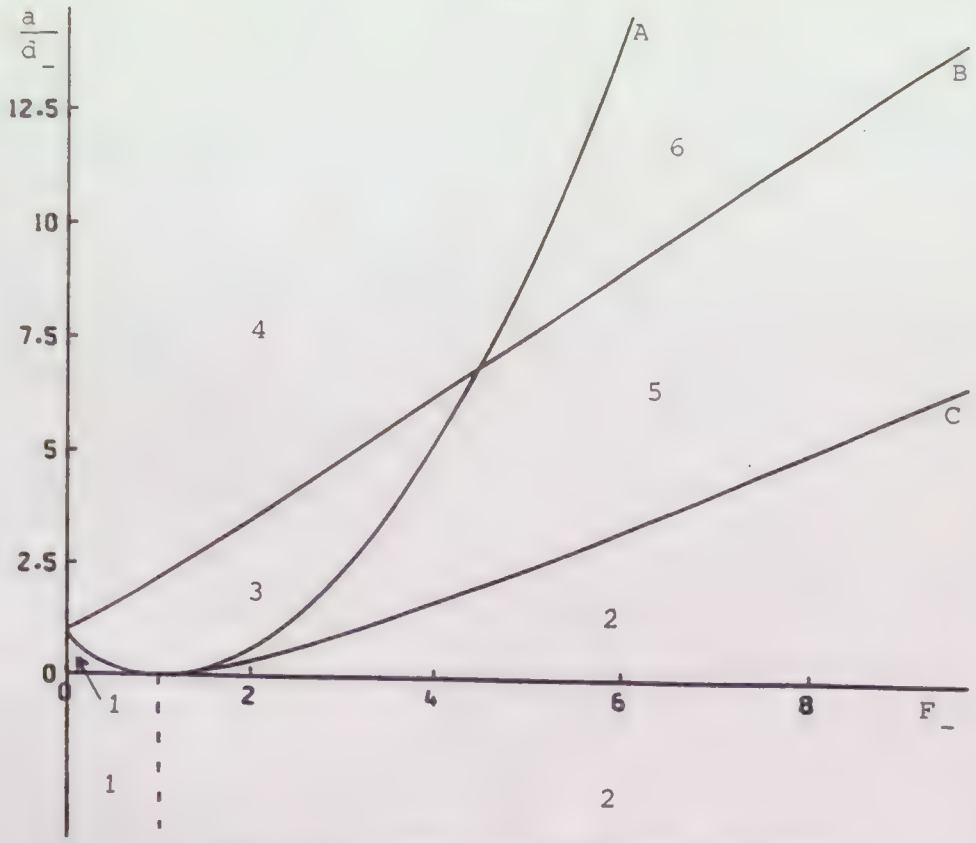

Fig. 16 Summary of solution domains

$$\frac{a}{d_-} = \frac{1}{2}\left[\frac{F_-}{\lambda_1}\right]^2 + \lambda_1 - \frac{3}{2}F_-^{2/3},$$

and elimination of λ_1 recovers (62). Points in Fig. 16 above C have the property $\lambda_2 > \lambda_1$, and points below C satisfy $\lambda_2 < \lambda_1$.

Points in Fig. 16 which are internal to the regions marked 1, 2, 3, 4, 5, 6 represent the following types of flow. We recall that, to be definite, our investigation has considered only flows in which the fluid velocities are everywhere to the right when non-zero and in which bores, when present, are upstream of the obstacle and (unless hydraulic jumps) are moving to the left away from it. Other solutions, in which the direction of motion of the fluid and/or the bore is different, or with a bore or hydraulic jump located elsewhere, can be sought using the same

principles of local analysis which we have set out in these papers. It may be possible to add them to Fig. 16.

1. Subcritical free flow, by (7) with $F_- < 1$. Also, the flow could meet a bore having strength within the range (56), each of which will induce an outgoing subcritical free flow.
2. Supercritical free flow, by (7) with $F_- > 1$. Also, the flow could meet a bore having strength within the range $\lambda_1 < \lambda < \lambda_0$ by (55), or a hydraulic jump with strength λ_1, each of which will induce an outgoing subcritical free flow.
3. Blocked flow, by (9), but relievable by a family of bores described in Theorem 2. Each bore converts the incoming flow, whether it be subcritical or supercritical, to a subcritical outgoing one. The bore of least strength λ_2 induces a branched flow. Stronger bores induce a free flow. Figs. 11 and 12 illustrate these cases.
4. Blocked flow, by (9), which is not relievable, by Theorem 2(i). In other words, there is no flow among the types currently under consideration.
5. Supercritical free flow, by (7). Also, because this region is not only below A, but below B and above C, the property $\lambda_1 < \lambda_2 < \lambda_0$ holds; it follows from (55) that the incoming supercritical flow could meet a bore with strength in the range $\lambda_2 \leq \lambda < \lambda_0$, which would induce an immediately subcritical outgoing flow which either branches (if $\lambda = \lambda_2$) at the apex or is free (if $\lambda > \lambda_2$).
6. Supercritical free flow only. This region is below A, and above both B and C, so that $\lambda_1 < \lambda_0 < \lambda_2$. The hypothesis (54) is violated since $d_-\lambda_0 < a$, and so the bores admitted by Theorem 5 are not available.

The three different parts of A itself represent the following types of flow.

4/6. Supercritical branched flow only.

3/5. Supercritical branched flow. Also, by Theorem 4, the supercritical incoming flow could meet a bore of strength $\lambda_2 = \lambda_3$ which converts it into another branched flow, as illustrated in Fig. 14, or into a free subcritical flow if the bore has greater strength than the minimum.

1/3. Subcritical branched flow. Also, by Theorem 4, the subcritical incoming flow could meet a bore which converts it into a free subcritical outgoing flow.

The two different parts of B itself represent the following types of flow.

3/4. Unrelievable blocking, by Theorem 2(i) because $\lambda_0 d_- = a$. The incoming flow is converted by the bore into a stagnant reservoir as explained for B after (61).

5/6. Supercritical free flow. Also, the free flow could be blocked by a bore which converts it into a stagnant reservoir as just explained. This phenomenon is in contrast to that within region 3, where a blocked flow is relieved by a bore.

Curve C is the boundary 2/5. Points on it can represent a supercritical free flow. Also, as we explained above, such an incoming flow can meet a hydraulic jump which converts it to a branched flow.

The boundary 1/2 is that between subcritical and supercritical incoming flows in which there is a hole in the bed. The flow could be free. It could also meet one of a family of bores described by Fig. I10(c), with strength in the range $1 < \lambda < \lambda_0$. Such a bore will induce an outgoing subcritical free flow.

Existing classification diagrams in the literature are confined to a small rectangle near the origin in Fig. 16, namely $0 \leq F_{-} \leq 2.5$, $0 \leq a/d_{-} \leq 1.25$ approximately. Therefore they omit important features which our detailed local analysis has revealed, such as the presence of region 6 and the intersection of curves A and B. We have also exhibited new flows within regions already known, such as in region 2. As we remarked above, the sensitivity to the shape of the obstacle apex, and the presence of smooth bifurcations in the flow there, are other new features demonstrated here.

REFERENCES

Baines, P.G. (1984) *A unified description of two-layer flow over topography*. J. Fluid Mech. 146, 127-167.

Baines, P.G. (1987) *Upstream blocking and airflow over mountains*. Ann. Rev. Fluid Mech. 19, 75-97.

Baines, P.G. and Davies, P.A. (1980) *Laboratory studies of topographic effects in rotating and/or stratified fluids*. Orographic effects in planetary flows. WMO GARP Publ. Ser. 23, 233-299.

Broad, A.S., Porter, D. and Sewell, M.J. (1991) *A new approach to shallow flow over an obstacle I: General theory*. Reading University Mathematics Department Report, 54 pp.

Durran, D.R. and Klemp, J.B. (1987) *Another look at downslope winds. Part II: Nonlinear amplification beneath wave-overturning layers*. J. Atmos. Sci. 44. 3402-3412.

Gill, A.E. (1977) *The hydraulics of rotating-channel flow*. J. Fluid. Mech. 80, 641-671.

Houghton, D.D. and Kasahara, A. (1968) *Nonlinear shallow fluid flow over an isolated ridge*. Comm. Pure and Appl. Math. 21, 1-23.

Huppert, H.E. (1980) *Topographic effects in stratified fluids*. Fjord Oceanography, H.J. Freeland, D.M. Farmer, and C.D. Levings, Eds., Plenum Press, New York, N.Y., 117-140.

Lawrence, G.A. (1987) *Steady flow over an obstacle*. J. Hydraulic Engng. 113, 981-991.

Long, R.R. (1954) *Some aspects of the flow of stratified fluids II: Experiments with a two-fluid system*. Tellus 6, 97-115.

Long, R.R. (1970) *Blocking effects in flow over obstacles.* Tellus 22, 471-480.

Long, R.R. (1972) *Finite amplitude disturbances in the flow of inviscid rotating and stratified fluids over obstacles.* Ann. Rev. Fluid Mech. 4, 69-92.

Pratt, L.J. (1983) *A note on nonlinear flow over obstacles.* Geophys. Astrophys. Fluid Dyn. 24, 63-68.

Pratt, L.J. (1984) *On nonlinear flow with multiple obstructions.* J. Atmos. Sci. 41, 1214-1225.

SHORT RANGE FORECASTING DIVISION SCIENTIFIC PAPERS

This is a new series to be known as Short Range Forecasting Division Scientific Papers . These will be papers from all three sections of the Short Range Forecasting Research Division i.e. Data Assimilation Research (DA),Numerical Modelling Research (NM), and Observations and Satellite Applications (OB) the latter being formerly known as Nowcasting (NS). This series succeeds the series of Short Range Forecasting Research /Met O 11 Scientific Notes.

1. **THE UNIFIED FORECAST /CLIMATE MODEL .**
   M.J.P. Cullen
   September 1991

2. **Preparation for the use of Doppler wind lidar information in meteorological data assimilation systems**
   A.C. Lorenc, R.J. Graham, I. Dharssi, B. Macpherson, N.B. Ingleby, R.W. Lunnon
   February 1992

3. **Current developments in very short range weather forecasting.**
   B.J. Conway
   March 1992

4. **DIAGNOSIS OF VISIBILITY IN THE UK MET OFFICE MESOSCALE MODEL AND THE USE OF A VISIBILITY ANALYSIS TO CONSTRAIN INITIAL CONDITIONS**
   S.P. Ballard, B.J. Wright, B.W. Golding
   April 1992

5. **Radiative Properties of Water and Ice Clouds at Wavelengths Appropriate to the HIRS Instrument**
   A.J. Baran and P.D. Watts
   2nd June 1992

6. **Anatomy of the Canonical Transformation**
   M.J. Sewell and I. Roulstone
   27 June 1992

7. **Hamiltonian Structure of a Solution Strategy for the Semi-Geostrophic Equations**
   I. Roulstone and J. Norbury
   29 June 1992

8. **Assimilation of Satellite Data in models for energy and water cycle Research**
   A.Lorenc
   July 1992

9. **The use of ERS-1 data in operational meteorology**
   A.Lorenc and others
   July 1992

10. **Bayesian quality control using multivariate normal distributions**
    N.B. Ingleby and A. Lorenc
    July 1992

11. **A NEW APPROACH TO SHALLOW FLOW OVER AN OBSTACLE**
    I General Theory
    A.S. Broad, D. Porter and M.J. Sewell
    10 August 1992

12. **A NEW APPROACH TO SHALLOW FLOW OVER AN OBSTACLE**
II Plane Flow over a Monotonic Mountain
A.S. Broad, D. Porter and M.J. Sewell
10 August 1992